MNRAS **000**, 000–000 (0000) Preprint 9 November 2016 Compiled using MNRAS LATEX style file v3.0

On the influence of the environment on galactic chemical abundances

L. S. Pilyugin[1,2], E. K. Grebel[2], I. A. Zinchenko[1,2], Y. A. Nefedyev[3], L. Mattsson[4]
[1] *Main Astronomical Observatory of National Academy of Sciences of Ukraine, 27 Zabolotnogo str., 03680 Kiev, Ukraine*
[2] *Astronomisches Rechen-Institut, Zentrum für Astronomie der Universität Heidelberg, Mönchhofstr. 12–14, 69120 Heidelberg, Germany*
[3] *Kazan Federal University, 18 Kremlyovskaya St., 420008, Kazan. Russian Federation*
[4] *Nordita, KTH Royal Institute of Technology & Stockholm University, Roslagstullsbacken 23, SE-106 91, Stockholm, Sweden*

arXiv:1611.02502v1 [astro-ph.GA] 8 Nov 2016

Accepted 2016 November 1. Received 2016 October 29; in original form 2016 August 23

ABSTRACT

We examine the influence of the environment on the chemical abundances of late-type galaxies with masses of $10^{9.1}$ $M_\odot$ – 10^{11} $M_\odot$ using data from the Sloan Digital Sky Survey (SDSS). We find that the environmental influence on galactic chemical abundances is strongest for galaxies with masses of $10^{9.1}$ $M_\odot$ to $10^{9.6}$ $M_\odot$. The galaxies in the densest environments may exceed the average oxygen abundances by about ∼ 0.05 dex (the median value of the overabundances for 101 galaxies in the densest environments) and show higher abundances in nitrogen by about ∼ 0.1. The abundance excess decreases with increasing galaxy mass and with decreasing environmental density. Since only a small fraction of late-type galaxies is located in high-density environments these galaxies do not have a significant influence on the general X/H – *M* relation. The metallicity – mass relations for isolated galaxies and for galaxies with neighbours are very similar. The mean shift of non-isolated galaxies around the metallicity – mass relation traced by the isolated galaxies is less than ∼ 0.01 dex for oxygen and less than ∼ 0.02 dex for nitrogen. The scatter in the galactic chemical abundances is large for any number of neighbour galaxies (at any environmental density), i.e., galaxies with both enhanced and reduced abundances can be found at any environmental density. This suggests that environmental effects do not play a key role in evolution of late-type galaxies as was also concluded in some of the previous studies.

Key words: galaxies: abundances – ISM: abundances – H II regions

1 INTRODUCTION

Establishing the parameters that govern the (chemical) evolution of galaxies is very important for understanding their formation and evolution. Lequeux et al. (1979) have shown that the metallicity in a galaxy correlates with its mass. The existence of a metallicity – mass (or metallicity – luminosity) relation at the present epoch and at different redshifts has been confirmed in many investigations (Lequeux et al. 1979; Zaritsky, Kennicutt & Huchra 1994; Garnett 2002; Grebel et al. 2003; Tremonti et al. 2004; Erb et al. 2006; Cowie & Barger 2008; Maiolino et al. 2008; Guseva et al. 2009; Thuan et al. 2010; Pilyugin & Thuan 2011; Pilyugin et al. 2013; Andrews & Martini 2013; Zahid et al. 2013; Maier et al. 2014; Steidel et al. 2014; Izotov et al. 2015, among many others). Nonetheless, the scatter in the abundances X/H at a given galaxy mass suggests that there may be additional parameters affecting galactic chemical evolution.

The gas-phase metallicity of galaxies with higher present-day star formation rates tends to be lower at a given stellar mass (Ellison et al. 2008; Zhang et al. 2009; Lara-López et al. 2010; Mannucci et al. 2010; Bothwell et al. 2013, among others). This can be easily understood from the following consideration. The abundance excess in a galaxy indicates that that galaxy has a higher astration level (and, consequently, a lower gas mass fraction) in comparison to the average galaxy (with zero abundance excess) at that stellar mass. Since the star formation rate decreases with decreasing amount of gas (e.g., Kennicutt 1998; Daddi et al. 2010; Kennicutt & Evans 2012) the star formation rate in galaxies with an abundance excess should be lower in comparison to standard galaxies of given stellar mass. It is difficult to consider the star formation rate as an independent parameter that governs the chemical evolution of galaxies. In general, the star formation history of a galaxy is defined by its mass.

The distribution of galaxies in the universe forms a complex network known as the cosmic web, comprising clusters, groups, filaments, walls, and voids (e.g., Zeldovich, Einasto & Shandarin 1982; de Lapparent, Geller, & Huchra 1986; Bond et al. 1996; Alpaslan et al. 2014). There are also very large overdense structures. The largest overdense structures in the nearby universe (the Shapley supercluster or Shapley concentration, the Great Attractor, and the Sloan Great Wall) include thousands of galaxies (Shapley 1930; Lynden-Bell et al. 1988; Gott et al. 2005; Sheth & Diaferio 2011). The dependence of galaxy properties on environment has

© 0000 The Authors

been considered in many papers. There is a well-defined relation between the local density of galaxies and the relative numbers of different morphological types. This morphology-density relation extends over five orders of magnitude in density in the sense that the fraction of spiral and irregular galaxies decreases with increasing density (e.g., Dressler 1980; Poggianti et al. 1999; van der Wel 2008). On the one hand, this implies that the environment affects the star formation history of galaxies. On the other hand, it was found that only the fraction of the star-forming galaxies depends on the environment while the star formation rates of the star-forming galaxies are similar in the highest and lowest density environments (Balogh et al. 2004; Brough et al. 2013; Wijesinghe et al. 2012; Beygu et al. 2016).

An influence of the environment on galaxy evolution should result in a dependence of galactic metallicity on environment. Many studies have been devoted to the investigation of the dependence of galactic chemical abundances on galactic environment (Shields et al. 1991; Vílchez 1995; Skillman et al. 1996; Pilyugin et al. 2002; Mouhcine et al. 2007; Ellison et al. 2009; Hughes et al. 2013; Peng & Maiolino 2014; Pustilnik et al. 2013; Nicholls et al. 2014; Darvish et al. 2015; Kacprzak et al. 2015; Kreckel et al. 2015; Shimakawa et al. 2015; Valentino et al. 2015, among many others), but no firm, unanimous conclusion has been reached. In fact, recent studies arrived at contradictory results. Kacprzak et al. (2015) found that there is no discernible difference between the mass – metallicity relation of field and cluster galaxies to within 0.02 dex. Shimakawa et al. (2015), on the other hand, established that cluster galaxies tend to be more chemically enriched than their field counterparts. In contrast, Valentino et al. (2015) suggest that star-forming galaxies in clusters are more metal-poor than their field counterparts. Gupta et al. (2016) investigated two galaxy clusters at redshifts z ~0.35. They found that the mass-metallicity relation for one cluster had an offest of 0.2 dex to higher metallicity compared to the local reference sample at a fixed mass. The median offsets in metallicity for galaxies in the other cluster is within the errors bars of the observations.

Our study of the dependence of galactic metallicity on its environment is motivated by the following. The present-day metallicity of a star-forming galaxy is usually specified by the oxygen abundance in the interstellar medium, because oxygen is the most abundant heavy element in the interstellar medium, because its abundance can be easily measured via emission lines when the gas is ionized, and because the majority of the methods for abundance determinations were developed for the measurement of oxygen abundances. Recently, we obtained a new calibration that provides estimates of the oxygen and nitrogen abundances in star-forming regions with high precision over the whole metallicity scale (Pilyugin & Grebel 2016). The mean difference between the strong-line based and T_e-based abundances is less than 0.05 dex for both oxygen and nitrogen. Since at 12 + log(O/H) $\gtrsim$ 8.2, secondary nitrogen becomes dominant and the nitrogen abundance increases at a faster rate in comparison to the oxygen abundance (Pagel 1997; Henry et al. 2000) the change in nitrogen abundance has a larger amplitude than the one in oxygen abundance and, as a consequence, may be easier to detect. Our present investigation is based on accurate oxygen and nitrogen abundances in a large sample of SDSS galaxies.

We will use the following standard notations for the line intensities:

$R_2 = I_{[\mathrm{O\,II}]\lambda3727+\lambda3729}/I_{\mathrm{H}\beta}$,
$N_2 = I_{[\mathrm{N\,II}]\lambda6548+\lambda6584}/I_{\mathrm{H}\beta}$,
$S_2 = I_{[\mathrm{S\,II}]\lambda6717+\lambda6731}/I_{\mathrm{H}\beta}$,
$R_3 = I_{[\mathrm{O\,III}]\lambda4959+\lambda5007}/I_{\mathrm{H}\beta}$.

The Sun's mass is used as the unit for the masses of galaxies.

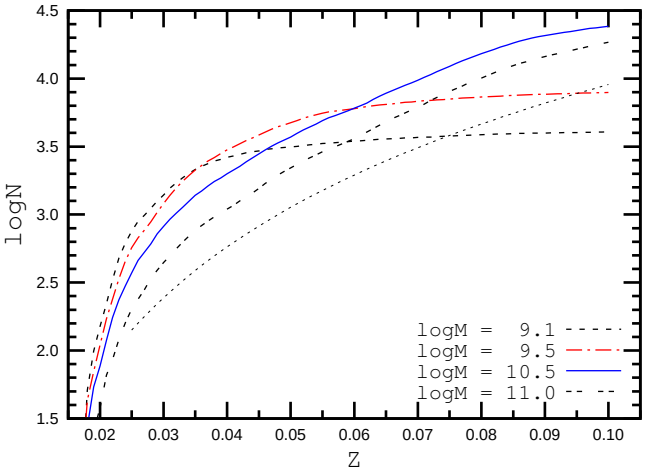

Figure 1. Cumulative number of galaxies with a redshift less than a given value. The curves for galaxies of four different values of the stellar mass are shown. The dotted curve shows the cumulative number of galaxies as a function of redshift for the case of constant galaxy space density.

2 DATA

Thanks to deep, wide-field sky surveys the number of galaxies with multi-wavelength data including spectra has increased considerably in recent years. In particular, numerous galaxies were measured by the Sloan Digital Sky Survey, SDSS, (York et al. 2000; Stoughton et al. 2002; Ahn et al. 2012). Our investigation relies on the SDSS data base (data release 12, DR12; (Alam et al. 2015)). An important task in our investigation is to select target galaxies with reliable data (especially regarding masses and abundances) and to reject the unreliable ones.

2.1 Our sample of "environment galaxies", S_{EG}

The positions, redshifts, and stellar masses of 2,235,900 galaxies were extracted from the SDSS data base (DR12, (Alam et al. 2015)). We adopted the spectral determination of the stellar masses of these galaxies provided by the SDSS. This sample of galaxies is used for the estimation of the environmental density and will be referred to as the sample of "environment galaxies", S_{EG}.

Fig. 1 shows the cumulative number of galaxies with a redshift less than a given value. The curves for galaxies of four different values of their stellar mass are shown. For each fixed value of log M_j the number of galaxies within a mass interval from log M_j-0.05 to log M_j+0.05 is determined. The dotted curve shows the cumulative number of galaxies as a function of redshift for the case of constant galaxy space density. The shape of this curve is used as reference. The curve for galaxies of a given mass follows to this shape until it reaches the redshift where the sample of galaxies of this mass becomes incomplete, i.e., the comparison between the shape of this curve and the shape of the curve for galaxies of a given mass allows one to estimate the limiting redshift out to which the galaxy sample of given mass interval is complete. Inspection of Fig. 1 suggests that a realistic density of galaxies with a mass of $10^{9.1}$ $M_\odot$ can be

estimated out to a redshift of ∼0.035 only, while for galaxies of mass of $10^{10.5}$ $M_\odot$ it can be estimated out to $z \sim 0.1$.

Distances to the galaxies are calculated from

$$d = \frac{c}{H_0} \times z, \quad (1)$$

where d is the distance in Mpc, c the speed of light in km s^{-1}, and z the redshift. The value of the Hubble constant H_0 was adopted to be 72 km s^{-1} Mpc^{-1}. This value was derived by the *Hubble Space Telescope* Key Project to measure the Hubble constant (Freedman et al. 2001). The analysis of the Planck observations of temperature and polarization anisotropies of the cosmic microwave backgraund results in a similar value of the Hubble constant, between 67 and 68 km s^{-1} Mpc^{-1} (Ade et al. 2014, 2015), as does the recent combination of Cepheid and supernova Type Ia measurements for the local Hubble constant, yielding ∼ 73 km s^{-1} Mpc^{-1} (Riess et al. 2016).

2.2 Our sample of "target galaxies", S_{TG}

Unfortunately, reliable abundances cannot be determined for all the SDSS galaxies. The gas-phase oxygen and nitrogen abundances of a star-forming galaxy can be estimated from emission line spectra. Spectra of ∼ 620,000 galaxies with measurements of the necessary emission lines Hβ, Hα, [O II]$\lambda\lambda$3727,3729, [O III]λ5007, [N II]λ6584, [S II]λ6717 and [S II]λ6731 are available in SDSS DR12. We select a sample of galaxies with reliable estimates of chemical abundances and will examine the influence of the environment on their abundances. This sample of galaxies will be referred to as the sample of "target galaxies", S_{TG}. The sample of target galaxies is a subsample of environment galaxies, i.e. only a fraction of the SDSS galaxies (with reliable estimations of the abundances) is used as target galaxies while all the SDSS galaxies are used to determine the environment density.

We used the hydrogen lines Hβ and Hα for the de-reddening. Specifically, we corrected the emission-line fluxes for interstellar reddening using the theoretical Hα/Hβ ratio and the Whitford (1958) interstellar reddening law (adopting the approximation suggested by Izotov et al. (1994)). In several cases, the derived value of the extinction C(Hβ) is negative and has then been set to zero.

The other lines were used for the determination of the oxygen and nitrogen abundances through our calibration relations. Only the spectra where S/N > 3 for the relevant emission lines are considered. It should be noted, however, that we also used additional criterion to select galaxies with reliable oxygen and nitrogen abundances (see below). We then utilise the resulting abundances of this galaxy sample to examine the influence of the environment, i.e., galaxy density, on the galactic metallicities.

Galaxies with AGN-like spectra were excluded using the [N II]λ6584/Hα vs. [O III]λ5007/Hβ diagnostic diagram of Baldwin, Phillips, Terlevich (1981). We adopt the dividing line between H II region-like and AGN-like spectra suggested by Kauffmann et al. (2003).

The resulting sample of galaxies with reliable estimates of chemical abundances and stellar masses is needed in order to examine the influence of the environment density on the galactic metallicities. In the following, we analyse our sample of the target galaxies after excluding the galaxies with unreliable estimates of stellar mass and abundance.

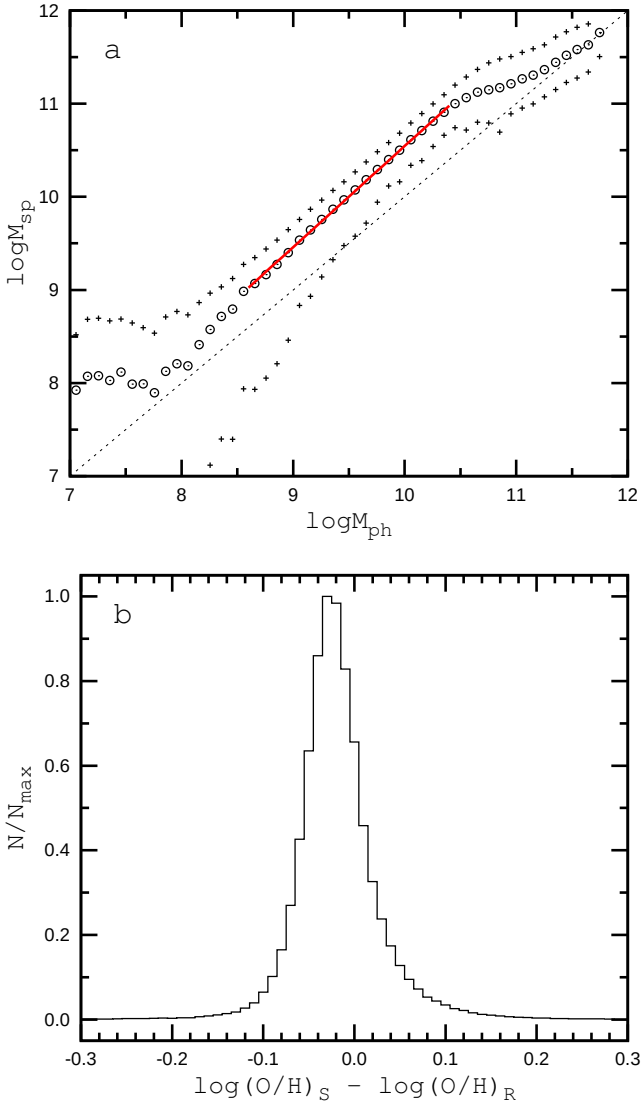

Figure 2. Upper panel: The value of the spectroscopically derived mass of a galaxy M_{sp} as a function of the photometrically inferred mass M_{ph}. The open circles are the mean values of log M_{ph} and log M_{sp} in bins of 0.1 in log M_{ph}, the plus signs are the mean deviations from the mean values. The solid line is the adopted relation between log M_{ph} and log M_{sp} within the mass interval from log M_{sp} = 9 to log M_{sp} = 11. The diagonal dotted line is the equal value line. The lower panel shows a normalised histogram of the differences between the R-calibration-based and S-calibration-based oxygen abundances log(O/H)$_S$ – log(O/H)$_R$ in our galaxies.

2.2.1 *The stellar masses of our galaxies*

The SDSS data base offers values of the stellar masses of galaxies determined in different ways. We have chosen the photometrical M_{ph} and spectral M_{sp} masses of the SDSS and BOSS galaxies (BOSS stands for the Baryon Oscillation Spectroscopic Survey in SDSS-III, see Dawson et al. (2013)). The photometric masses are the best-fit stellar masses from database table stellarMassStarformingPort obtained by the Portsmouth method, which fits stellar evolution models to the SDSS photometry (Maraston et al. 2009). The spectral masses are the median (50th percentile of the probability distribution function, PDF) of the logarithmic stellar masses from table stellarMassPCAWiscBC03 determined by the Wiscon-

sin method (Chen et al. 2012) with the stellar population synthesis models from Bruzual & Charlot (2003).

The upper panel of Fig. 2 shows the photometric mass M_{ph} as a function of the corresponding spectral mass M_{sp}. The range of galaxy masses is devided into bins of 0.1 dex in M_{ph}. For the galaxies within each bin, the mean values of log M_{ph} and log M_{sp} and the mean deviations from the mean values are determined. The mean values of log M_{ph} and log M_{sp} are shown in the upper panel of Fig. 2 by open circles, and the mean deviations by plus signs.

The upper panel of Fig. 2 shows that the values of log M_{ph} and log M_{sp} are roughly the same only for very massive galaxies and that there is a shift between log M_{ph} and log M_{sp} for galaxies of lower masses. It should be noted that Kannappan & Gawiser (2007) have demonstrated that different stellar mass estimation methods yield relative mass scales that can disagree by factor $\gtrsim 3$. The relation between log M_{ph} and log M_{sp} can be approximated by the linear relation

$$\log M^*_{sp} = 1.086 \log M_{ph} - 0.313 \quad (2)$$

for galaxies within the stellar mass interval $9 < \log M_{sp} < 11$. This relation can then be used to exclude galaxies with unreliable stellar masses within this interval. More precisely, we exclude the galaxies where the mean difference between log M^*_{sp} and log M_{sp} is larger than 0.2 dex.

If the difference between log M^*_{sp} and log M_{sp} can be interpreted as the random error of the stellar galaxy mass and the difference between log M_{ph} and log M_{sp} as a systematic error then the mean random error of the stellar galaxy mass for the sample of galaxies within the stellar mass interval $9 < \log M_{sp} < 11$ is ~0.11 dex and the systematic error can excess 0.5 dex.

In the following we will use the spectral masses of the galaxies and will denote them as M without an index.

2.2.2 *The chemical abundances of our galaxies*

The oxygen and nitrogen abundances of the galaxies of our sample are estimated using two calibrations from Pilyugin & Grebel (2016) where two sets of strong emission lines are used. The oxygen abundances $(O/H)_R$ are determined using the R_2, R_3, and N_2 line intensities

$$\begin{aligned}(O/H)^*_R &= 8.589 + 0.022\ \log(R_3/R_2) + 0.399\ \log N_2 \\ &+ (-0.137 + 0.164\ \log(R_3/R_2) + 0.589 \log N_2) \\ &\times \log R_2\end{aligned} \quad (3)$$

if $\log N_2 > -0.6$, and

$$\begin{aligned}(O/H)^*_R &= 7.932 + 0.944\ \log(R_3/R_2) + 0.695\ \log N_2 \\ &+ (0.970 - 0.291\ \log(R_3/R_2) - 0.019 \log N_2) \\ &\times \log R_2\end{aligned} \quad (4)$$

if $\log N_2 < -0.6$. The notation $(O/H)^* = 12 + \log(O/H)$ is used for the sake of the brevity.

The oxygen abundances $(O/H)_S$ are determined using the N_2, R_3, and S_2 line intensities

$$\begin{aligned}(O/H)^*_S &= 8.424 + 0.030\ \log(R_3/S_2) + 0.751\ \log N_2 \\ &+ (-0.349 + 0.182\ \log(R_3/S_2) + 0.508 \log N_2) \\ &\times \log S_2\end{aligned} \quad (5)$$

if $\log N_2 > -0.6$, and

$$\begin{aligned}(O/H)^*_S &= 8.072 + 0.789\ \log(R_3/S_2) + 0.726\ \log N_2 \\ &+ (1.069 - 0.170\ \log(R_3/S_2) + 0.022 \log N_2) \\ &\times \log S_2\end{aligned} \quad (6)$$

if $\log N_2 < -0.6$.

A normalised histogram of the differences between those values of the abundance $\log(O/H)_S - \log(O/H)_R$ is presented in the lower panel of Fig. 2. The scatter in the differences of oxygen abundances is rather small but there is a systematic shift of around −0.03 dex in the values of $\log(O/H)_S$ in comparison to the values of $\log(O/H)_R$. We determine the linear relation between $\log(O/H)_S$ and $\log(O/H)_R$

$$12 + \log(O/H)^c_R = 12 + \log(O/H)_S + 0.029 \quad (7)$$

and use this relation to exclude galaxies with unreliable estimations of oxygen abundance. The adopted selection criterion is the following. Galaxies where the absolute value of the difference between $\log(O/H)^c_R$ and $\log(O/H)_R$ exceeds 0.05 are excluded from the sample. This means that we exclude a galaxy if its emission line [O II]$\lambda\lambda$3727,3729 or/and its emission line [S II]$\lambda\lambda$6717,6731 measurements show large uncertainties. It should be emphasised that it is difficult to reveal the uncertainties in the measurements of the emission line [O III]$\lambda\lambda$4959,5007 and [N II]$\lambda\lambda$6548,6584 through comparison of the abundances $\log(O/H)_S$ and $\log(O/H)_R$ since those lines can contribute similar errors in both. Strictly speaking, we excluded only a fraction of galaxies with unreliable oxygen abundances.

Below only the oxygen abundances $(O/H)_R$ will be used, and we will refer to them as O/H.

The nitrogen abundances were estimated in two ways. First, the nitrogen abundances were obtained through the following relations (Pilyugin & Grebel 2016):

$$\begin{aligned}(N/H)^*_R &= 7.939 + 0.135\ \log(R_3/R_2) + 1.217\ \log N_2 \\ &+ (-0.765 + 0.166\ \log(R_3/R_2) + 0.449 \log N_2) \\ &\times \log R_2\end{aligned} \quad (8)$$

if $\log N_2 > -0.6$, and

$$\begin{aligned}(N/H)^*_R &= 7.476 + 0.879\ \log(R_3/R_2) + 1.451\ \log N_2 \\ &+ (-0.011 - 0.327\ \log(R_3/R_2) - 0.064 \log N_2) \\ &\times \log R_2\end{aligned} \quad (9)$$

if $\log N_2 < -0.6$. Again the notation $(N/H)^* = 12 + \log(N/H)$ is adopted for the sake of brevity.

Second, the nitrogen-to-oxygen abundance ratio N/O is estimated using the expression that relates the nitrogen-to-oxygen abundance ratio N/O in an H II region with the intensities of the strong lines in its spectrum,

$$\begin{aligned}\log(N/O) &= -0.657 - 0.201\ \log N_2 \\ &+ (0.742 - 0.075\ \log N_2) \times \log(N_2/R_2)\end{aligned} \quad (10)$$

and then the nitrogen abundance is determined using

$$\log(N/H) = \log(O/H) + \log(N/O) \quad (11)$$

where the oxygen abundance $(O/H)_R$ is used. The galaxies where the absolute value of the difference between two values of nitrogen abundances exceeds 0.05 dex are excluded from the sample (one more selection criterion).

Below, only nitrogen abundances estimated in the second way will be used, and we will refer to them as N/H.

2.2.3 *Metallicity – stellar mass diagram*

Our sample of target galaxies with stellar masses in the range of $9.1 < \log M < 11$ and redshifts $z < 0.1$ after excluding AGNs and galaxies with unreliable estimates of stellar masses and oxygen and nitrogen abundances amounts to 77,659 galaxies.

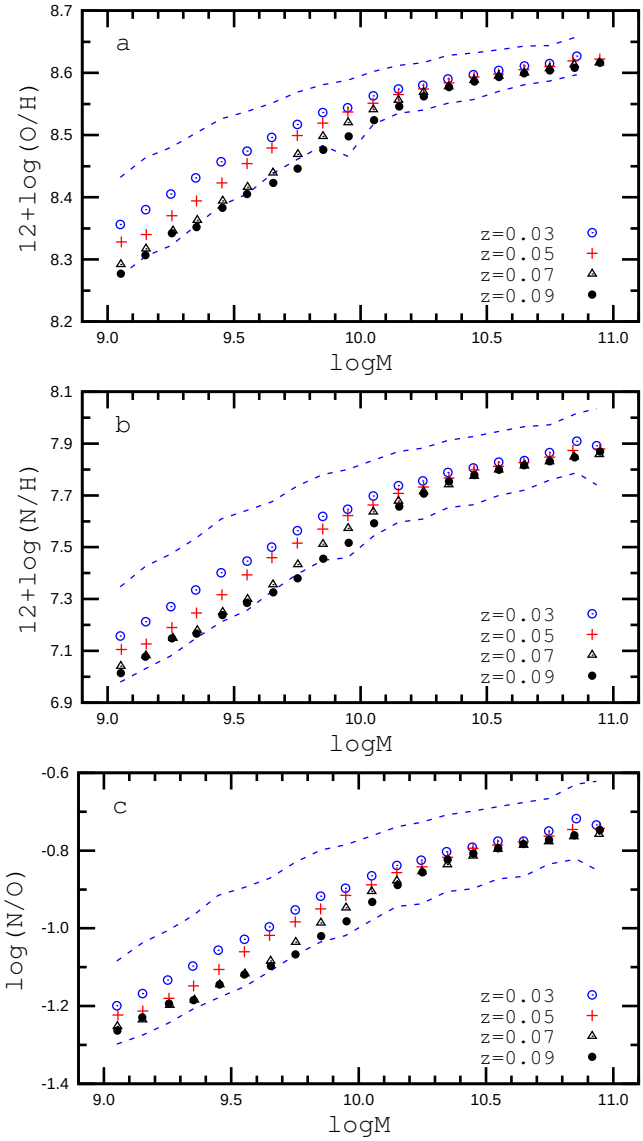

Figure 3. Panel *a*. The oxygen abundance vs. stellar mass diagram for our sample of target galaxies. The O/H – *M* relations for galaxies in four redshift intervals of $z \pm 0.01$ are presented. The symbols indicate the mean values for the bins of 0.1 dex in stellar masses. The dashed lines show the mean deviations for the subsample of galaxies with redshift $z = 0.03$. Panels *b* and *c* show the same as panel *a* but for nitrogen and nitrogen-to-oxygen ratio, respectively.

Panel *a* of Fig. 3 shows the O/H – *M* diagram for this sample of target galaxies. The O/H – *M* relations for galaxies in four redshift bins $z_j \pm 0.01$ (where $z_j = 0.03$, 0.05, 0.07, and 0.09) are presented. The symbols in Fig. 3 show the mean values in bins of 0.1 dex of the stellar masses. The O/H – *M* relations at low redshifts are more reliable for the low-mass galaxies than for the massive galaxies because the low-mass galaxies are numerous at low redshifts in our sample while the number of massive galaxies is rather low, see Fig. 1. Conversely, the O/H – *M* relations for large (near $z \sim 0.1$) redshifts are more reliable for massive galaxies than for the low-mass galaxies.

The dashed lines in panel *a* of Fig. 3 show the mean deviations of the oxygen abundances for the subsample of galaxies with redshift $z = 0.03$. Inspection of panel *a* of Fig. 3 shows that the change in the oxygen abundances in low-mass galaxies due to the evolution over the redshift diapason ~0.05 (over the time interval ~0.5 Gyr) is comparable to the scatter in abundances for galaxies at the fixed redshift $z = 0.03$. Therefore, a deviation of the abundance of an individual galaxy from the mass – metallicity relation can serve as indicator of overabundance (in particular, due to influence of the environment) if only the galaxies within a small diapason of redshift are considered, i.e. if the evolutionary effect on the galaxy oxygen abundance is excluded. The evolutionary change of the oxygen abundance in massive galaxies at the considered redshift interval is less pronounced.

Panels *b* and *c* show the same as panel *a* but for the nitrogen abundance and the nitrogen-to-oxygen abundances ratio, respectively. Again, the change in the nitrogen abundances and nitrogen-to-oxygen abundances ratio in low-mass galaxies due to the evolution over the time interval ~0.5 Gyr is comparable to the scatters for galaxies at the redshift $z = 0.03$.

The examination of the X/H – *M* diagrams in Fig. 3 reveals three major trends of galactic chemical abundances with mass and redshift.

(i). The oxygen abundance increases with increasing masses and with decreasing redshift. The X/H – *M* relation flattens at the massive end. This agrees with the mass-metallicity (or luminosity-metallicity) relation of galaxies revealed by Lequeux et al. (1979) and confirmed in the local universe and at high redshifts in many earlier studies (e.g., Zaritsky, Kennicutt & Huchra 1994; Garnett 2002; Grebel et al. 2003; Tremonti et al. 2004; Erb et al. 2006; Pilyugin et al. 2007; Maiolino et al. 2008; Guseva et al. 2009; Pilyugin et al. 2013; Maier et al. 2014; Izotov et al. 2015).

(ii). The rate of the change of oxygen abundances with redshift decreases with increasing galaxy masses. Gavazzi (1993) found that the present-day rate of evolution of late-type galaxies decreases with increasing mass, suggesting that the efficiency of conversion of gas into stars at an early epoch increases with the mass of the system. This effect has been named “downsizing” and has been confirmed in many studies (e.g., Cowie et al. 1996; Heavens et al. 2004; Maiolino et al. 2008; Tomczak et al. 2016).

(iii). The rate of the change of nitrogen abundance with redshift and stellar mass is higher than that for oxygen. The faster rate of the change of nitrogen abundances as compared to oxygen abundances above 12+ log(O/H) ~ 8.2 clearly demonstrates the rise of N/O in the N/O vs. O/H diagram considered in many studies (Edmunds & Pagel 1978; Izotov & Thuan 1999; Henry et al. 2000; Pilyugin et al. 2003, 2004; Berg et al. 2012; Annibali et al. 2015; Croxall et al 2016, among many others).

Since only a sample of galaxies within a rather small interval of redshifts (ages) are considered, the evolutionary changes in oxygen abundances are small, around 0.05 dex. Nevertheless, our X/H = $f(z, M)$ relations reproduce the known trends in galactic abundances. This can be considered as evidence that the precision of the derived abundances is high enough to allow us to detect abundance changes of the order of ~0.05 dex and below.

The SDSS spectra are measured through 3 arcsec diameter fibres and, consequently, at low redshifts the projected aperture diameter is smaller than that at high redshift. Since there is usually a radial abundance gradient in galaxy discs (see Vila-Costas & Edmunds 1992; Zaritsky, Kennicutt & Huchra 1994; van Zee et al. 1998; Pilyugin et al. 2004, 2006, 2014; Moustakas et al. 2010; Sánchez et al. 2014), an aperture-redshift effect can be present in abundances based on SDSS spectra (e.g.

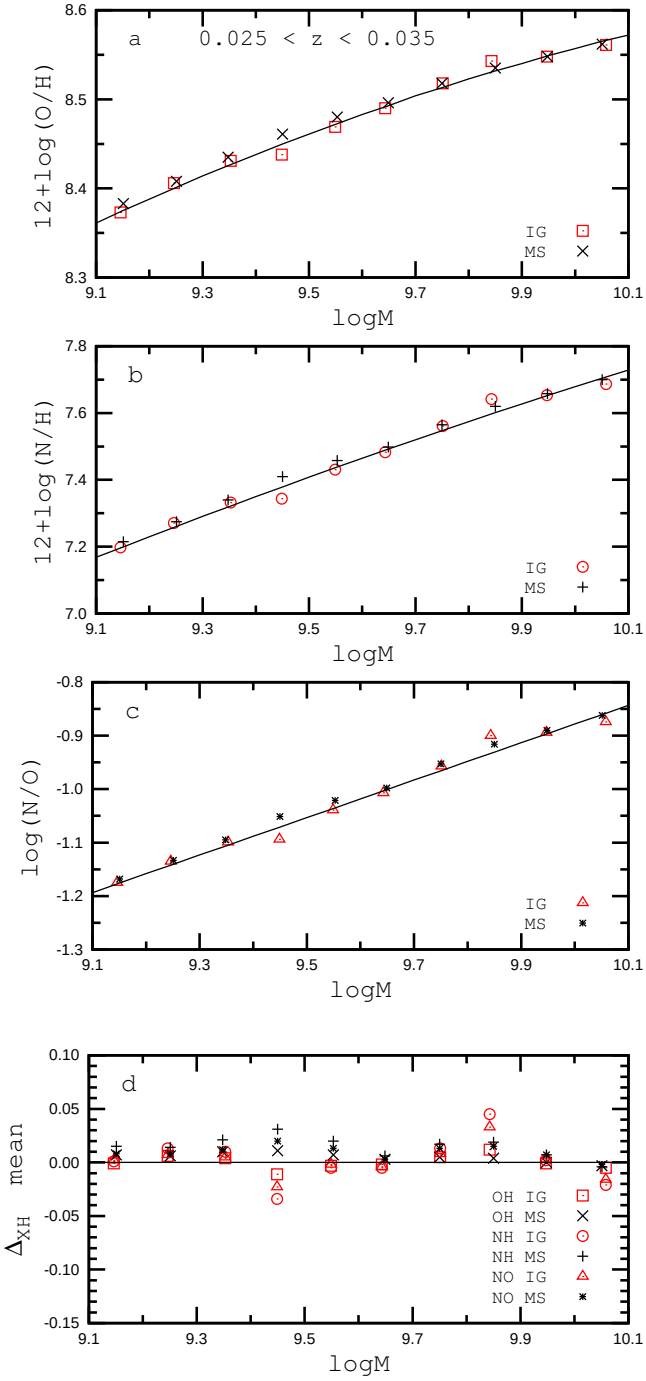

Figure 4. Comparison between the abundances of isolated galaxies (IGs) and galaxies with neighbours (multiple-system galaxies, MSs). Panel *a*. The solid line represents the O/H – *M* relation for IGs (Eq. 13). The squares show the mean oxygen abundances for the IGs in bins of 0.1 dex in stellar masses. The crosses indicate the mean oxygen abundances for MSs. Panel *b*. The solid line is the N/H – *M* relation for IGs (Eq. 14). The circles denote the mean nitrogen abundances for the IGs in bins of 0.1 dex in stellar masses. The plus signs mark the mean nitrogen abundances for MSs. Panel *c*. The solid line is the N/O – *M* relation for IGs (Eq. 15). The triangles are the mean nitrogen-to-oxygen abundance ratios for the IGs in bins of 0.1 dex in stellar masses. The asterisks show the mean nitrogen abundances for MSs. Panel *d*. The mean chemical overabundance of galaxies in bins of 0.1 dex in stellar masses. The overabundances in oxygen are shown by squares for the IGs and by crosses for the MSs. The overabundances in nitrogen are shown by circles for the IGs and by plus signs for the MSs. The deviations in nitrogen-to-oxygen ratio are shown by triangles for the IGs and by asterisks for the MSs.

Kewley et al. 2005). At low redshift the SDSS spectra are the spectra of the central parts of galaxies while at large redshift they are close to global spectra of whole galaxies, i.e. the abundances based on the SDSS spectra are more biased towards the central metallicity at low than at high redshifts. The aperture effect can contribute to the mass-dependent redshift evolution seen in Fig. 3. To exclude (or at least minimise) the aperture effect on the scatter in abundances, a sample of galaxies within a small interval of redshifts should be considered.

3 INFLUENCE OF THE ENVIRONMENT ON THE CHEMICAL ABUNDANCES IN GALAXIES

3.1 Environmental influence on the abundances in galaxies of masses of $10^{9.1}$ $M_\odot$ to $10^{10.1}$ $M_\odot$

We noted above that a realistic environmental density of galaxies of masses of log M = 9 can be estimated out to a redshift of $\sim$ 0.035 only (see Fig. 1). Here, we examine now the influence of the environment on the chemical abundances of target galaxies with redshifts from z = 0.025 to 0.035. Since the redshift interval is small the evolutionary change (i.e., change with redshift) of the abundance can be neglected. We will also restrict ourselves to the examination of target galaxies within the stellar mass range from log M = 9.1 to 10.1. On the one hand, those galaxies are the most numerous in our sample of the target galaxies at redshifts from z = 0.025 to 0.035. On the other hand, one can expect (see Fig. 3) that the X/H – M relations for the galaxies within this stellar mass interval can be well reproduced by a simple expression. This sample amounts to 4572 galaxies and will be referred to as sample *S* 030.

3.1.1 *Isolated galaxies vs. multiple systems*

We divide sample *S* 030 into two subsamples: the subsample of isolated galaxies (IG) and the subsample of multiple systems (MS), i.e., galaxies with neighbours. To select the isolated galaxies, a criterion based on a selection in a projected distance – velocity difference space is usually employed. However, different numerical values for such criteria are adopted in the literature (e.g., Fuse et al. 2012; Argudo-Fernández et al. 2015; Spector & Brosch 2016; Lacerna et al. 2016). We have chosen to use the isolation criteria from Lacerna et al. (2016). A galaxy is considered as an IG if it has no known neighbour within the projected separation across the line of sight R of less than 100 typical isophotal radii R_{25} and with a radial velocity difference ΔV less than 1000 km s^{-1}. We adopt the typical value of R_{25} for late-type galaxies to be 13 kpc (Pilyugin et al. 2014). Then the isolation criteria are

$$\begin{aligned} R &> 1.3 \text{ Mpc} \\ \Delta z &> 0.0033 \end{aligned} \qquad (12)$$

For each target galaxy from sample *S* 030, we search for neighbours in our sample of environment galaxies S_{EG}. It should be emphasised that only environment galaxies with masses higher than 10^9 $M_\odot$ were taken into account. 531 galaxies from the sample *S* 030 are isolated galaxies according to our isolation criteria.

For isolated galaxies, we obtain the O/H – M relation

$$12 + \log(\mathrm{O/H}) = 8.333 + 0.290\, m - 0.0658\, m^2, \qquad (13)$$

the N/H – M relation

$$12 + \log(\mathrm{N/H}) = 7.104 + 0.640\, m - 0.0660\, m^2, \qquad (14)$$

and the N/O – M relation

$$\log(\mathrm{N/O}) = -1.228 + 0.351\, m - 0.0003\, m^2, \qquad (15)$$

where $m = \log M - 9$. A few galaxies (14 out of 531) show large deviations from the O/H – M ($d_{OH} > 0.15$ dex) or from the N/H – M ($d_{NH} > 0.40$ dex) relations. Those galaxies are not used in deriving the final relations and are excluded from our further analysis. The mean deviation from the final relations (i.e., the mean value of the residuals in the relations)

$$d_{XH} = \left(\frac{1}{n} \sum_{j=1}^{n} (\log(\mathrm{X/H})_j^{OBS} - \log(\mathrm{X/H})_j^{CAL})^2 \right)^{1/2} \qquad (16)$$

is $d_{OH} = 0.058$ dex, $d_{NH} = 0.160$ dex, and $d_{NO} = 0.106$ dex for the remaining 517 isolated galaxies.

It is widely accepted that the mass – metallicity relation for galaxies is caused by the variation of the astration level (or gas mass fraction) with galaxy mass, in the sense that the astration level increases (gas mass fraction decreases) with increasing galaxy mass. The scatter in abundances among the galaxies of a given stellar mass evidences that there is a spread in the astration levels (or gas mass fractions) among those galaxies. Surely, the uncertainties in the stellar masses and the abunances may be responsible for the some fraction of the scatter in abundances. The variation with astration level is larger for nitrogen abundances than for oxygen because the secondary nitrogen is dominant at the metallicities in our sample of galaxies. As a consequence, the scatter in abundances among galaxies of a given mass due to the spread in the astration levels is larger for nitrogen than for oxygen. The time delay between nitrogen and oxygen enrichment together with the different star formation histories in galaxies can make an additional contribution to the scatter in the nitrogen abundances (e.g., Edmunds & Pagel 1978; Pagel 1997; Henry et al. 2000; Pilyugin & Thuan 2011).

Let us compare the agreement of the X/H – M diagrams for the isolated galaxies and for multiple system galaxies. The O/H – M relation obtained for the isolated galaxies of masses in the range $10.1 \gtrsim \log M \gtrsim 9.1$ at redshifts $0.035 \gtrsim z \gtrsim 0.025$ is shown by the solid line in panel *a* of Fig. 4. The squares represent the mean oxygen abundances for IGs in bins of 0.1 dex in stellar mass. The crosses show the mean oxygen abundances for MSs. We refer to the difference between the measured abundance and the abundance obtained from the X/H – M relation as "overabundance". The mean chemical overabundance of a subsample of galaxies is defined by

$$\Delta_{XH} = \frac{1}{n} \sum_{j=1}^{n} (\log(\mathrm{X/H})_j^{OBS} - \log(\mathrm{X/H})_j^{CAL}) \qquad (17)$$

where X/H = O/H or X/H = N/H. The mean oxygen overabundances Δ_{OH} in bins of 0.1 dex in stellar mass are shown by squares for the IGs and by crosses for the MSs in panel *d* of Fig. 4. The values of Δ_{OH} in the bins depend on the choice of the bin size and are used for illustration only. The oxygen overabundance averaged over all MSs specifies the mean shift of the abundances in MSs from the OH – M relation traced by the isolated galaxies. The mean oxygen overabundance for all (3900) MSs is $\Delta_{OH} = 0.0055$.

The solid line in panel *b* of Fig. 4 is the obtained N/H – M relation. The circles mark the mean nitrogen abundances for IGs in bins of 0.1 dex in stellar masses. The plus signs denote the mean oxygen abundances for MSs. The overabundances in nitrogen are shown by circles for IGs and by plus signs for MSs in panel *d* of Fig. 4. The mean nitrogen overabundance for all MSs is $\Delta_{NH} = 0.0155$. It should be noted that Kacprzak et al. (2015) have also recently found that there is no discernible difference between the mass – metallicity relation of field and cluster galaxies to within 0.02 dex.

The solid line in panel *c* of Fig. 4 is the obtained N/O – M relation. The triangles are the mean N/O ratios for IGs in bins of 0.1 dex in stellar masses. The asterisks denote the nitrogen-to-oxygen ratios for MSs. The N/O deviations are shown by triangles for IGs and by asterisks for MSs in panel *d* of Fig. 4. The mean N/O deviation for all MSs is $\Delta_{NH} = 0.0100$.

Thus, the general metallicity – mass relations for isolated galaxies and galaxies having neighbours are close to each other. The mean shift of non-isolated galaxies around the metallicity – mass relation traced by the isolated galaxies is less than ~ 0.01 dex for oxygen and less than ~ 0.02 dex for nitrogen. This suggests that environmental effects do not play a key role in the chemical evolution of galaxies.

3.1.2 *Chemical overabundance in galaxies as a function of number of neighbours*

Here we examine whether chemical overabundances in a galaxy depend on the number of neighbour galaxies, i.e., on the environmental density.

The environmental density of a galaxy can be quantified in different ways. Here it will be specified by the number of galaxies within a region of a certain projected distance – velocity difference space. The number of galaxies in the region is determined using neighbourhood criteria defined in a way similar to the isolation criteria. A galaxy is considered to be a neighbour of the target galaxy if it has the projected separation across the line of sight of less than a fixed value R_0 and a redshift difference less than a fixed value dz_0. Five different values of R_0 are considered: $R_0 = 1$ Mpc, 2 Mpc, 3 Mpc, 4 Mpc, and 5 Mpc. Each value of R_0 is accompanied by a value of dz_0 that involves two components. The first component corresponds to the change of redshift with distance equal to the adopted R_0. The second component takes the peculiar velocities of galaxies, V_p, into account. Thus, the total value of dz_0 is the sum $dz_0 = dz_0(R_0) + dz_0(V_p)$. Three values of peculiar velocities V_p are considered: $V_p = 1000$ km s^{-1}, 500 km s^{-1}, 100 km s^{-1}.

Let us first discuss the case of $V_p = 1000$ km s^{-1}. For each target galaxy from sample $S\,030$, we count the number of neighbour galaxies in the sample of the environment galaxies S_{EG}. The panels in the left column of Fig. 5 show the mean oxygen overabundances as a function of the number of neighbour galaxies within the regions defined by R_0 specified in each panel. The target galaxies are divided into bins according to the number of neighbour galaxies. The bin sizes are 2 for $R_0 = 1$ Mpc, 5 for $R_0 = 2$ Mpc, 10 for $R_0 = 3$ Mpc, 15 for $R_0 = 4$ Mpc, and 20 for $R_0 = 5$ Mpc. The mean oxygen overabundances Δ_{OH} are determined for the target galaxies in each bin and shown in the panels in the left column of Fig. 5 by the filled circles. The solid line is the linear best fit to all the individual galaxies (not to the bin means shown in the figure). The scatter in the overabundances among galaxies in the bin is specified by the mean deviation of the overabundances $d(\Delta_{\mathrm{OH}})$. The separate deviations above and below the mean value of the overabundance are calculated if the number of galaxies with deviations above (below) is at least 3. The mean deviations of the overabundances are shown by plus signs in the panels of the left column of Fig. 5.

The panels of the middle column of Fig. 5 show the logarithm of the number of target galaxies having a given number of neighbour galaxies. Inspection of these panels suggests that there is some

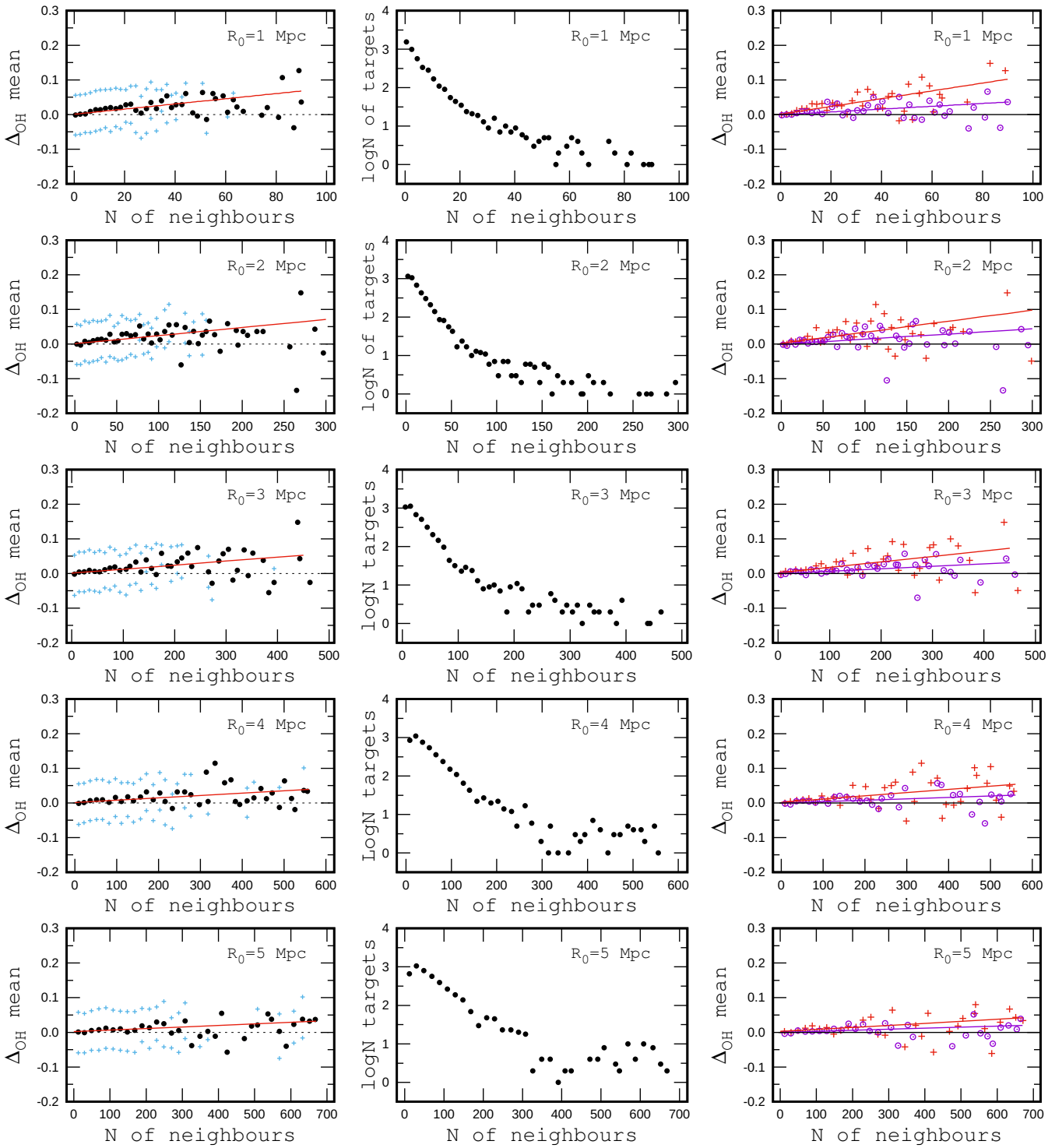

Figure 5. Left column: Mean oxygen overabundance Δ_{OH} (black points) and mean deviation (blue plus signs) of the target galaxies with stellar masses of $9.1 \lesssim \log M \lesssim 10.1$ at redshifts $0.025 \lesssim z \lesssim 0.035$ as a function of the number of neighbour galaxies for different values of R_0 as labeled in each panel. The solid line is the linear best fit to all the individual data points. The value of the peculiar velocities of the neighbouring galaxies is adopted to be equal to 1000 km s^{-1}. The mean values are obtained for galaxies in bins of the number of neighbouring galaxies. The bins are 2 for $R_0 = 1$ Mpc, 5 for $R_0 = 2$ Mpc, 10 for $R_0 = 3$ Mpc, 15 for $R_0 = 4$ Mpc, and 20 for $R_0 = 5$ Mpc. Middle column: The logarithm of the number of target galaxies having a given number of neighbour galaxies. Right column: The circles indicate the mean oxygen overabundance of galaxies of $9.6 < \log M < 10.1$ and the solid line is the linear best fit. The plus signs show the mean oxygen overabundance of galaxies of masses $9.1 < \log M < 9.6$ and the dashed line is the linear best fit.

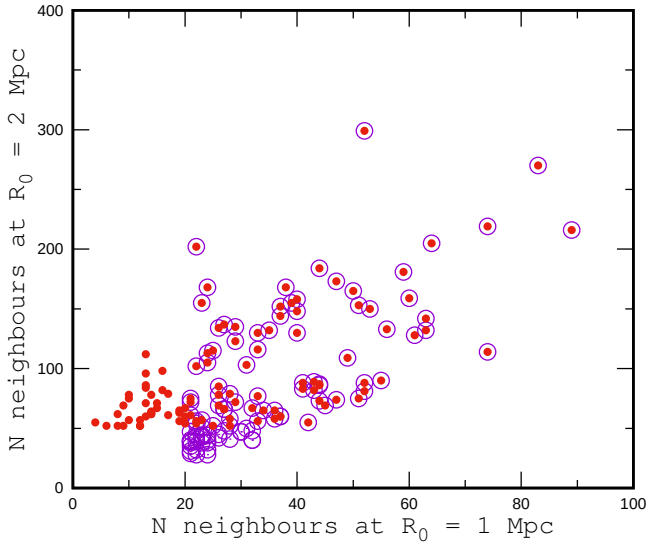

Figure 6. The relation between the number of neighbour galaxies at $R_0 = 2$ Mpc and at $R_0 = 1$ Mpc for galaxies of $9.1 < \log M < 9.6$. The circles visualise data for 111 galaxies with numbers of neighbour galaxies at $R_0 = 1$ Mpc higher than 20. The points show data for 113 galaxies with numbers of neighbour galaxies at $R_0 = 2$ Mpc higher than 51.

influence of the environment on the abundances, i.e., the galaxies in the dense environments tend to have an overabundance of oxygen.

Fig. 5 suggests that the oxygen overabundance in galaxies in dense local environments (at $R_0 = 1$ Mpc) is higher than that of galaxies in dense extended environments (at $R_0 = 5$ Mpc), i.e., the oxygen overabundance is more sensivite to the local than to the extended environment density.

Is the influence of the environment on the galactic chemical abundances similar for galaxies of different masses? We have divided the sample of target galaxies *S* 030 into two subsamples: the "low-mass galaxies" of stellar masses of $9.1 < \log M < 9.6$ and "high-mass galaxies" with masses of $9.6 < \log M < 10.1$. The mean oxygen overabundances Δ_{OH} are determined for those subsamples separately. The panels in the right column of Fig. 5 show the mean oxygen overabundance Δ_{OH} of the high-mass galaxies (circles) and low-mass galaxies (plus signs) as a function of the number of the neighbour galaxies. The linear best fit to the data for the high-mass galaxies is shown by the dashed line and that for low-mass galaxies by the solid line. Inspection of the panels in the right column of Fig. 5 suggests that the influence of the environment on the abundances depends on galaxy mass, in the sense that the low-mass galaxies show higher oxygen overabundance than the high-mass galaxies.

We use the median value of the overabundances for the 101 galaxies with the densest environments at $R_0 = 1$ Mpc. The median value of the oxygen overabundance and the scatter in the overabundances is 0.053 ± 0.067 dex for galaxies with masses of $9.1 < \log M < 9.6$ and 0.017 ± 0.045 dex for galaxies with masses of $9.6 < \log M < 10.1$.

Are the regions with the densest local environments (at $R_0 = 1$ Mpc) also associated with high-density environments on larger scales? Fig. 6 shows the relation between the number of neighbour galaxies at $R_0 = 2$ Mpc and at $R_0 = 1$ Mpc for galaxies of $9.1 < \log M < 9.6$. The circles represent data for 111 galaxies with more than 20 neighbour galaxies within $R_0 = 1$ Mpc. The points denote data for 113 galaxies with more than 51 neighbour galaxies within $R_0 = 2$ Mpc. Fig. 6 shows that the sample of regions with the densest local environments at $R_0 =\sim 1$ Mpc and the sample of regions with the densest environments at $R_0 = 2$ Mpc overlap only partly. The regions with the densest local environments (at $R_0 = 1$ Mpc) are not necessarily associated with the highest-density regions on larger scales. The regions with high-density local environments can be found both in low-density and high-density extended environments.

So, there is an influence of the environment on the galactic metallicities, i.e., the galaxies in dense environments tend to have an overabundance in oxygen. The influence of the environment on the abundances depends on galaxy mass, in the sense that the low-mass galaxies tend to show higher oxygen overabundances than the high-mass galaxies. However, the scatter in the oxygen overabundances is large at any environmental density, i.e., galaxies with both enhanced and reduced oxygen abundances can be found at any density of the environment. These conclusions can be checked using the nitrogen abundances. It was noted above that the secondary nitrogen becomes dominant at 12+ log(O/H) $\gtrsim 8.2$, and, as consequence, the nitrogen abundance increases at a faster rate in comparison to the oxygen abundance (Pagel 1997; Henry et al. 2000). One can therefore expect that the overabundance in nitrogen should have a larger amplitude than that for oxygen.

The panels in the left column of Fig. 7 show the mean nitrogen overabundances (points) and mean deviations of the overabundances (plus signs) as a function of the number of neighbour galaxies. The panels in the middle column show the logarithm of the number of target galaxies with a given number of neighbour galaxies. The panels in the right column Fig. 7 show the mean nitrogen overabundance Δ_{NH} of the high-mass galaxies (circles) and low-mass galaxies (plus signs) as a function of the number of neighbour galaxies.

Comparing Fig. 5 and Fig. 7 shows that the general behavior of the oxygen and nitrogen overabundances is similar. Again there is a tendency that the galaxies in dense environments are on average more nitrogen-rich than other galaxies. The nitrogen overabundance is most appreciable for low-mass galaxies in the densest environments and decreases with increasing galaxy mass and decreasing environment density. The median values of the nitrogen overabundances and their scatter for the 101 galaxies with the densest environments within $R_0 = 1$ Mpc are 0.109 ± 0.172 dex for galaxies with masses of $9.1 < \log M < 9.6$ and 0.077 ± 0.152 dex for galaxies in the mass range of $9.6 < \log M < 10.1$. As expected, the overabundances in nitrogen are higher than the ones in oxygen.

The left panels of Fig. 8 show the mean N/O excess (points) and mean deviations of the excesses (plus signs) as a function of the number of neighbour galaxies. The middle panels show the logarithm of the number of target galaxies with a given number of neighbour galaxies. The right panels of Fig. 8 show the mean excess Δ_{NO} of the high-mass galaxies (circles) and low-mass galaxies (plus signs) as a function of the number of neighbour galaxies. Comparison of Fig. 5, Fig. 7 and Fig. 8 shows that the general behavior of the N/O excesses is similar to that for oxygen and nitrogen overabundances.

Thus, the nitrogen abundances in our galaxies confirm the conclusions reached from the analysis of the oxygen abundances.

It was noted above that different numerical values of the peculiar galactic velocities V_p were adopted in different studies (e.g., Fuse et al. 2012; Argudo-Fernández et al. 2015; Spector & Brosch 2016; Lacerna et al. 2016). Above we considered the case of $V_p = 1000$ km s^{-1}. To evaluate the influence of the adopted value of the peculiar velocities on the results, we considered different values for

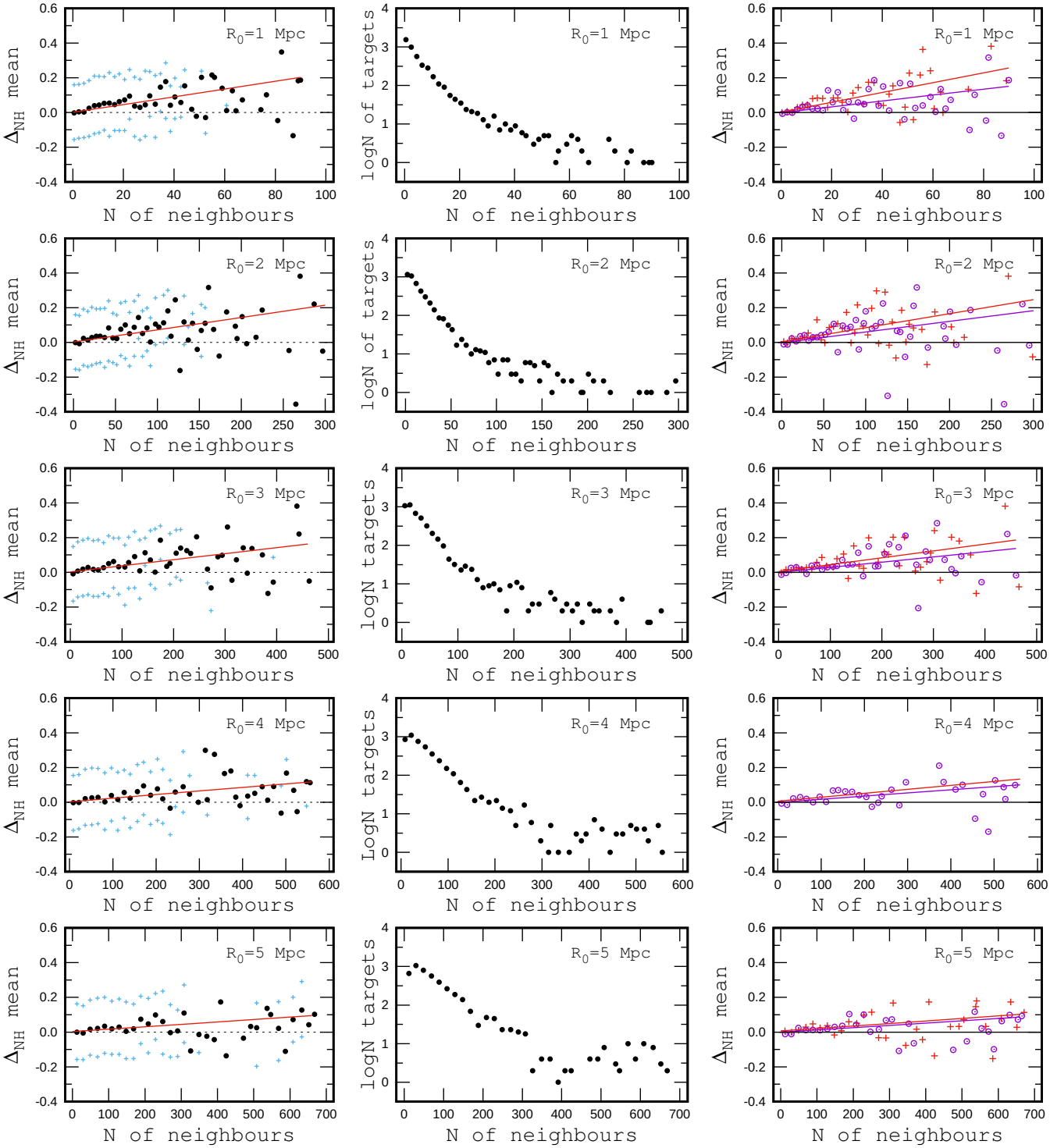

Figure 7. The same as Fig. 5 but for nitrogen.

this quantity. The results for the peculiar velocities V_p = 100 km s^{-1} are presented in Fig. 9. The panels in the left column of Fig. 9 show the mean oxygen overabundances (points) and mean deviations of the overabundances (plus signs) as a function of the number of the neighbouring galaxies for the five values of R_0 given in each panel. However, the bin sizes differ from the ones used for V_p = 1000 km s^{-1}. Here the bin sizes in the number of neighbour galaxies are 1 for R_0 = 1 Mpc, 3 for R_0 = 2 Mpc, 5 for R_0 = 3 Mpc, 8 for R_0 = 4 Mpc, and 10 for R_0 = 5 Mpc. The panels in the middle column show the logarithm of the number of target galaxies having a given number of neighbouring galaxies. The panels in the right column of Fig. 9 show the mean oxygen overabundance Δ_{OH} of the high-mass (circles) and low-mass galaxies (plus signs) as a function of the number of neighbour galaxies.

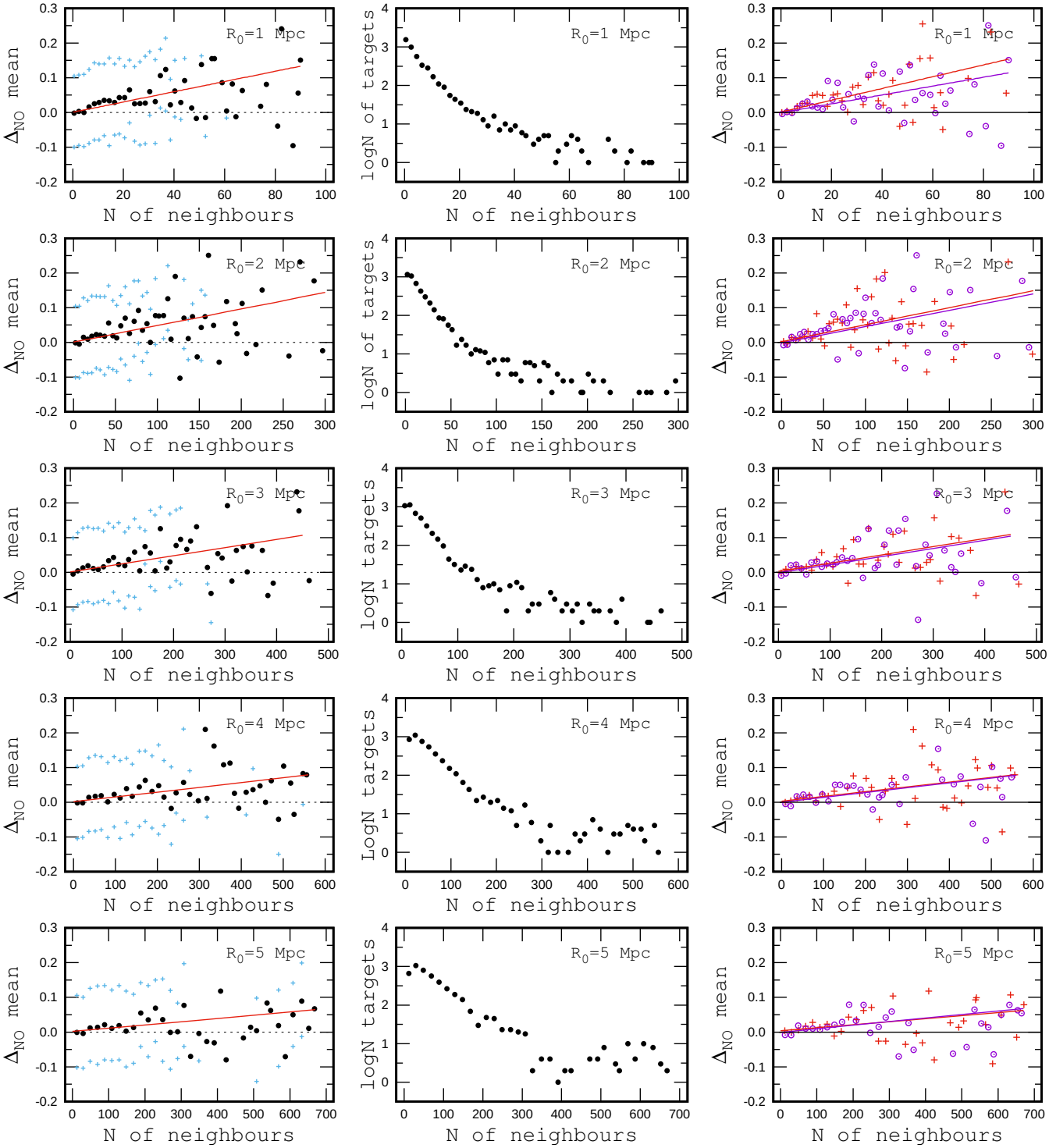

Figure 8. The same as Fig. 5 but for nitrogen-to-oxygen ratio.

The comparison between Fig. 5 and Fig. 9 llustrates that the general behavior of the oxygen overabundances is similar for V_p = 1000 km s^{-1} and V_p = 100 km s^{-1}. Again there is a tendency that the galaxies in the dense environment are on average more oxygen-rich than other galaxies. The overabundances decreases with increasing galaxy mass and with decreasing environmental density. It is not surprising that the number of neighbouring galaxies in the case of V_p = 1000 km s^{-1} is larger than that for V_p = 100 km s^{-1}.

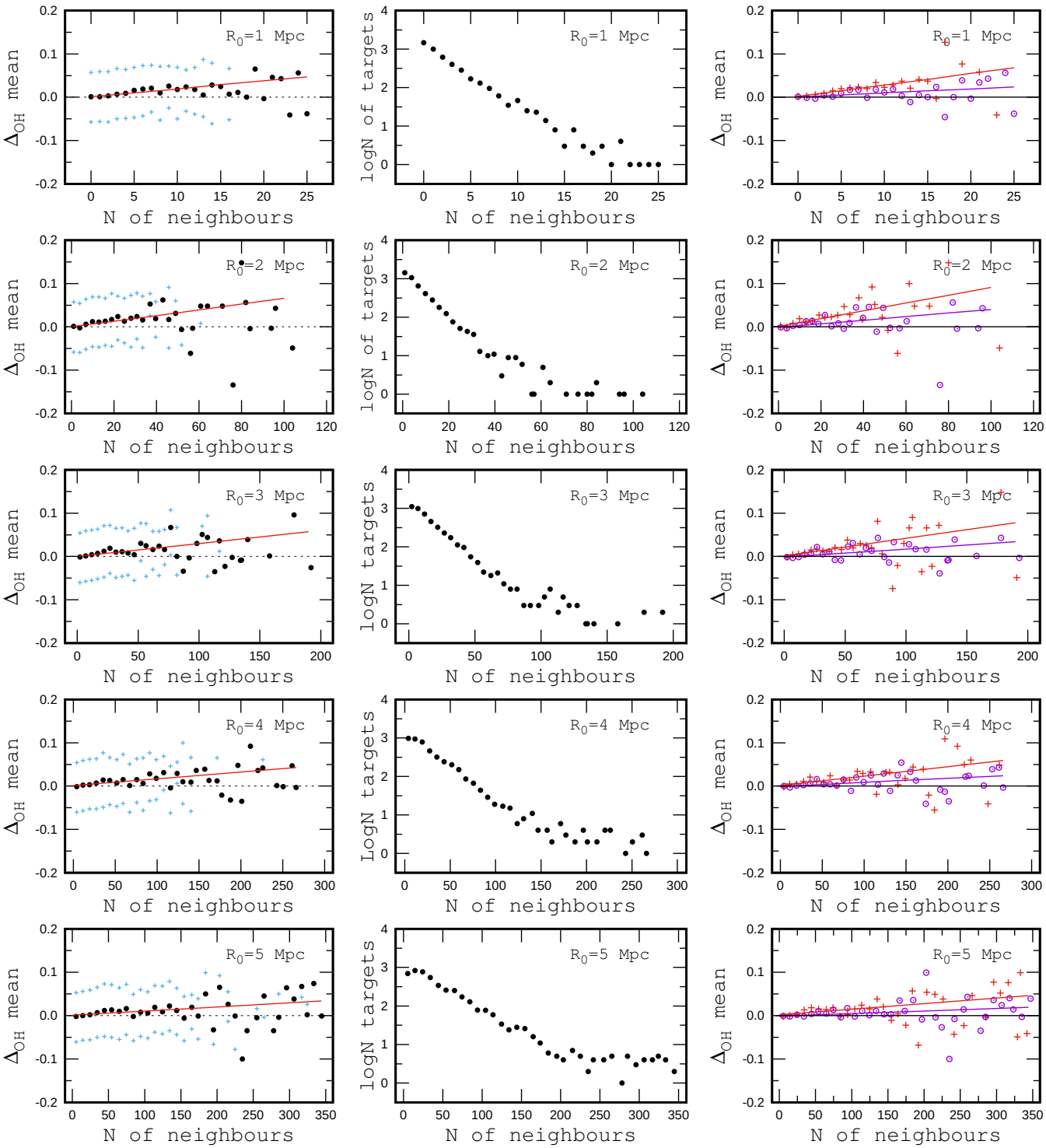

Figure 9. The same as Fig. 5 but for the value of the peculiar velocities of the neighbour galaxies of 100 km s^{-1}.

3.2 Environmental influence on the abundances in galaxies of masses of $10^{10.5}$M$_\odot$ to 10^{11}M$_\odot$

We showed in Section 2.1 that a realistic (complete) environmental density of galaxies with masses of log$M$ $\sim$ 10.5 can be estimated out to a redshift of $\sim$ 0.1, see Fig. 1. Here we examine the influence of the environment on the abundances of target galaxies with redshifts ranging from z = 0.06 to 0.10. The environmental density is estimated as the number of neighbouring galaxies with masses higher than log$M \gtrsim$ 10.5.

We consider the target galaxies in the stellar mass range from log$M$ = 10.5 to 11. We again neglect the evolutionary change of the chemical abundances, i.e., the dependence of the abundances on redshift. Fig. 3 suggests that the X/H – M relations for the galaxies

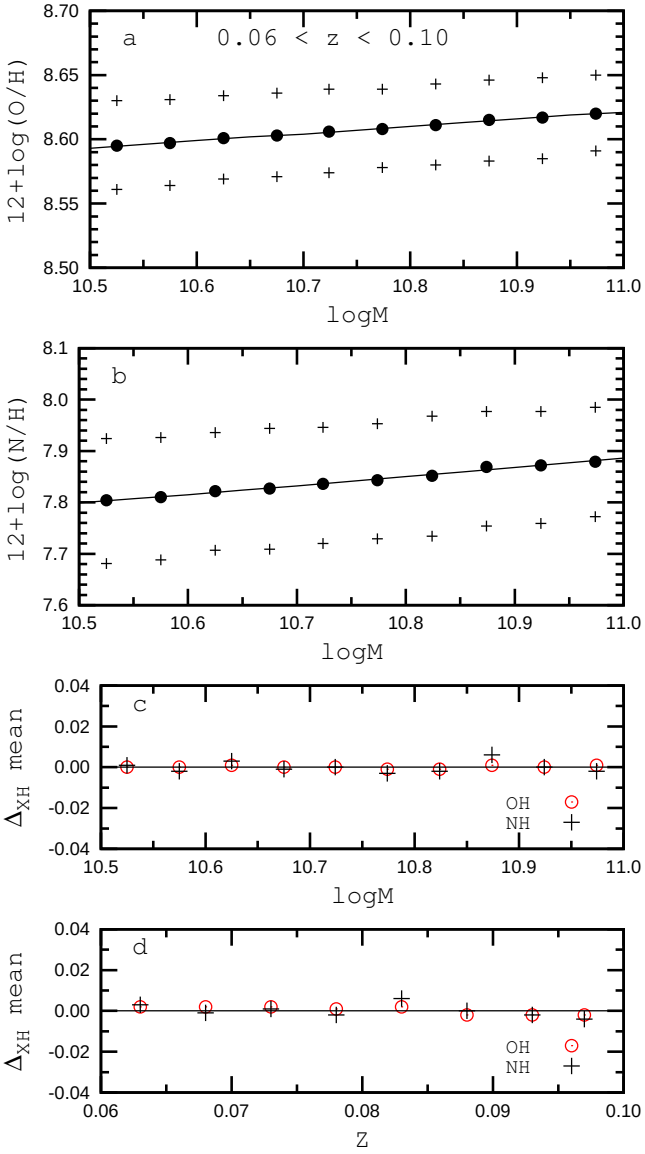

Figure 10. X/H – M relations for the sample of galaxies with masses of $10.5 < \log M < 11$ and redhifts of $0.06 < z < 0.1$. Panel *a*. The solid line shows the O/H $-M$ relation The points represent the mean oxygen abundances for galaxies in bins of 0.05 dex in stellar masses. The plus signs indicate the mean deviations of the oxygen abundance for the galaxies in the bins. Panel *b*. The same as Panel *a* but for nitrogen abundance. Panel *c*. The mean over(under)abundance of oxygen (points) and nitrogen (plus signs) averaged for the galaxies in bins of 0.05 dex in stellar mass as a function of galaxy mass. Panel *d*. The mean over(under)abundance of oxygen (points) and nitrogen (plus signs) averaged for galaxies in bins of 0.005 in redshift as a function of redshift.

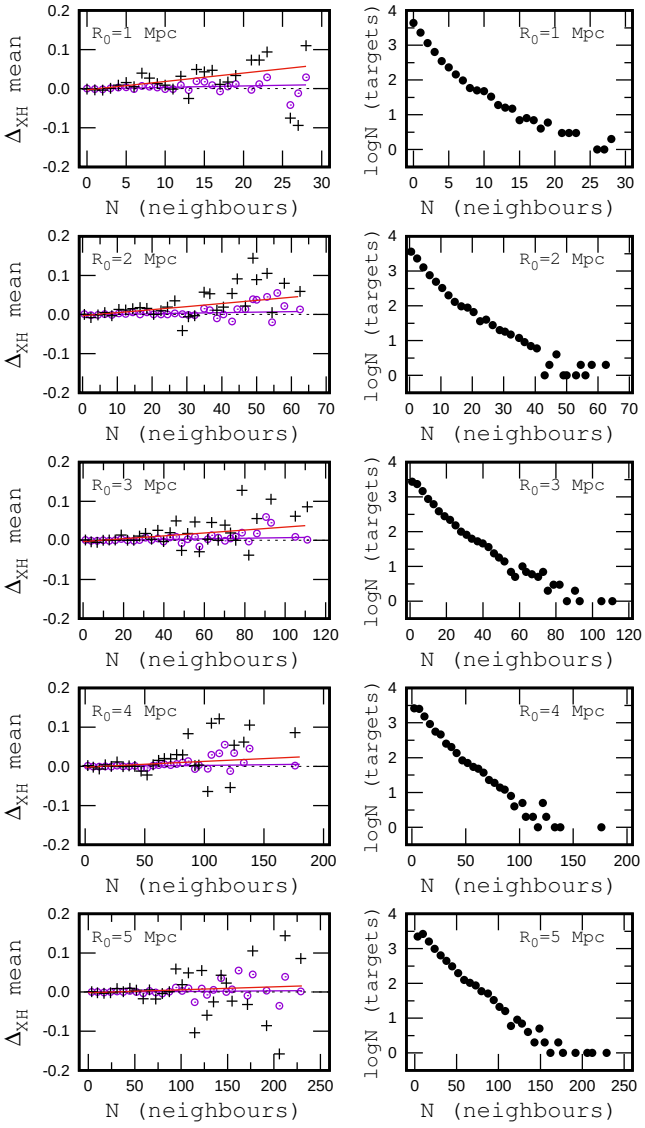

Figure 11. Panels in the left column: Mean overabundance $d_{\rm XH}$ of galaxies with redshifts of $0.6 \lesssim z \lesssim 0.1$ and stellar masses of $10.5 \lesssim \log M \lesssim 11$ as a function of number of neighbour galaxies within the radius R_0 labeled in each panel. The value of the peculiar velocities of the neighbour galaxies is adopted to be 1000 km s^{-1}. The mean overabundances in oxygen (circles) and nitrogen (plus signs) are estimated for galaxies binned according to their number of neighbour galaxies. The bins are 1 for $R_0 = 1$ Mpc, 2 for $R_0 = 2$ Mpc, 3 for $R_0 = 3$ Mpc, 5 for $R_0 = 4$ Mpc, and 7 for $R_0 = 5$ Mpc. The panels in the right column show the logarithm of the number of target galaxies having a given number of neighbour galaxies.

within this stellar mass interval can be reproduced by a simple expression. Since we consider only massive galaxies here we cannot correctly extract isolated galaxies. Hence, we determine the O/H – M relation for all galaxies of sample $S\,100$. The resulting O/H – M relation is

$$12 + \log({\rm O/H}) = 8.565 + 0.055\,m + 0.00071\,m^2, \qquad (18)$$

and the N/H – M relation is

$$12 + \log({\rm N/H}) = 7.725 + 0133\,m + 0.027\,m^2 \qquad (19)$$

where $m = \log M - 10$. The galaxies with large deviations from the O/H – M relation ($d_{O/H} > 0.15$ dex) or from the N/H – M relation ($d_{N/H} > 0.4$ dex) are not used in deriving the final relations and are excluded from further analysis (332 galaxies out of 9896). The mean deviations are $d_{OH} = 0.032$ dex and $d_{NH} = 0.118$ dex based on 9564 galaxies. Thus, our sample of target galaxies with redshifts in the range of $0.10 \gtrsim z \gtrsim 0.06$ and stellar masses of $11 \gtrsim \log M \gtrsim 10.5$ consists of 9564 galaxies and will be referred to as sample $S\,100$. This sample of galaxies includes the galaxies from the very large overdense structure known as the Sloan Great Wall (Gott et al. 2005; Sheth & Diaferio 2011).

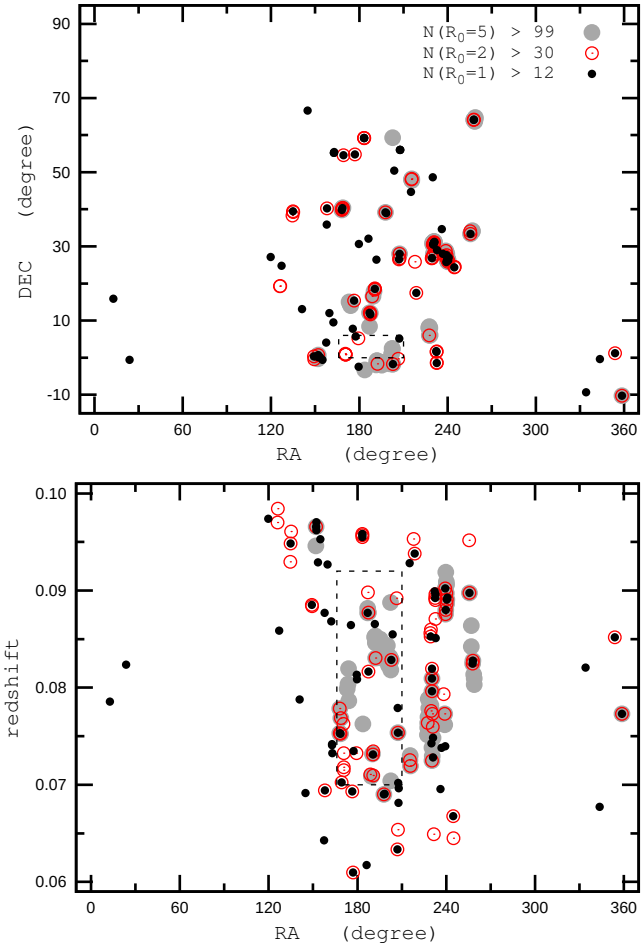

Figure 12. Upper panel: Coordinate map of the galaxies from the sample $S100$ with the densest environment. The points stand for galaxies for which the number of neighbours at $R_0 = 1$ Mpc is larger than 12, the dark open circles depict galaxies for which the number of neighbours within $R_0 = 2$ Mpc is larger than 30, and the grey filled circles indicate galaxies for which the number of neighbours within $R_0 = 5$ Mpc is larger than 99. The dashed line is roughly outlines the position of the Sloan Great Wall. The lower panel shows the location of the galaxies from the upper panel in the RA vs. redshift plane. The symbols are the same as in the upper panel.

The obtained O/H – M relation is shown in panel *a* of Fig. 10 by the solid line. The filled circles indicate oxygen abundances of galaxies averaged in bins of 0.05 dex in stellar mass. The plus signs mark the mean deviations of the oxygen abundance $d_{\rm OH}$ for those galaxies. The N/H – M relation is shown in panel *b* of Fig. 10 by the solid line. Again the filled circles denote nitrogen abundances averaged for galaxies in bins of 0.05 dex in stellar mass, and the plus signs indicate the mean deviations of the nitrogen abundance $d_{\rm NH}$. Panel *c* of Fig. 10 shows the mean over(under)abundances of oxygen $\Delta_{\rm OH}$ (circles) and nitrogen $\Delta_{\rm NH}$ (plus signs) for galaxies in stellar mass bins of 0.05 dex as a function of galaxy mass, and panel *d* shows the mean over(under)abundances of oxygen (circles) and nitrogen (plus signs) in redshift bins of 0.005 as a function of redshift. Panel *d* of Fig. 10 demonstrates that there is no appreciable trend of mean overabundance of oxygen and nitrogen with redshift. This confirms our assumption that the evolutionary change of abundances (i.e., the dependence of the abundances on redshift) for our sample of galaxies can be neglected.

For each target galaxy we count the number of neighbouring galaxies in the sample of environment galaxies S_{EG}. The number of galaxies in the region is determined using the neighbourhood criteria defined earlier. Again the five different values of $R_0 = 1$ Mpc, 2 Mpc, 3 Mpc, 4 Mpc, and 5 Mpc are considered. Only the case of a peculiar velocity of $V_p = 1000$ km s^{-1} is discussed.

The panels in the left column of Fig. 11 show the mean oxygen (circles) and nitrogen (plus signs) overabundance as a function of the number of neighbouring galaxies within the volume defined by the value of R_0 given in each panel. The solid line shows the best fit to the oxygen data and the dashed line to the nitrogen data. The panels in the right column show the logarithm of the number of the target galaxies having the given number of neighbouring galaxies. The oxygen overabundances show a marginal (in fact, negligibly small) correlation with the environmental density while the trend with nitrogen overabundances is more noticeable. The median value of the overabundance and scatter in the overabundances for the 101 galaxies with the densest environment at $R_0 = 1$ Mpc is 0.002 ± 0.035 dex for oxygen and 0.041 ± 0.120 dex for nitrogen. A comparison of Fig. 5 and Fig. 11 as well as of the median values of the overabundances confirms the general trend that the overabundances of galaxies in high-density environments decrease with increasing galaxy mass.

We also consider the case of peculiar velocities of $V_p = 100$ km s^{-1}. The general behavior of the oxygen and nitrogen overabundances is similar for cases where $V_p = 1000$ km s^{-1} and $V_p = 100$ km s^{-1} are used to count the number of neighbouring galaxies. Again the trend of overabundances with the environmental density is insignificant for oxygen but more notable for nitrogen overabundances.

Our sample involves the galaxies from the large overdense structure called the Sloan Great Wall. This permits us to take a closer look at the distributions of the regions of the densest environments. The upper panel in Fig. 12 shows a sky map of galaxies with the densest environments. The black filled circles mark the galaxies with the densest local environments, i.e., galaxies for which the number of neighbours at $R_0 = 1$ Mpc is larger than 12. The dark (red) open circles denote galaxies for which the number of neighbours at $R_0 = 2$ Mpc is larger than 30. The grey filled circles indicate the galaxies with the densest extended environments, i.e., galaxies for which the number of neighbours at $R_5 = 5$ Mpc is larger than 99. The lower panel shows the location of those galaxies in the R.A. – z plane. The Sloan Great Wall is roughly outlined by the dashed line stretching from R.A. ∼ 166° to R.A. ∼ 210° and from Dec ∼ 0 to Dec ∼ 6° at redshifts from $z \sim 0.07$ to ∼ 0.092 (Gott et al. 2005; Sheth & Diaferio 2011).

Fig. 12 reveals that the high-density regions at scales of 5 Mpc show a concentration (clustering) with several centres including the Sloan Great Wall. The high-density regions at scales of 1 – 2 Mpc show a more uniform distribution in space and do dot exhibit a significant concentration to the Sloan Great Wall. We again found that the regions of the densest local environments (at $R_0 = 1$ Mpc) are not nesessarily associated with the regions of the densest environments at larger scales and the regions of the high-density local environments can be found both in low-density and high-density extended environments.

4 DISCUSSION

The effects of the environment on the metal content of late-type galaxies has been debated for a long time (Shields et al.

1991; Vílchez 1995; Skillman et al. 1996; Pilyugin et al. 2002; Mouhcine et al. 2007; Ellison et al. 2009; Hughes et al. 2013; Peng & Maiolino 2014; Pustilnik et al. 2013; Nicholls et al. 2014; Darvish et al. 2015; Kacprzak et al. 2015; Kreckel et al. 2015; Shimakawa et al. 2015; Valentino et al. 2015, among many others).

These studies focus on comparisons between cluster and field galaxies. For instance, Shields et al. (1991) determined the abundances in five Virgo spirals of type Sc and found evidence that spiral galaxies in the Virgo cluster have systematically higher interstellar abundances than comparable field galaxies.

Vílchez (1995) examined the influence of the environment on the evolution of dwarf galaxies. Subsamples of dwarf galaxies in nearby voids, in the field of the local supercluster, and in the direction of the core of the Virgo cluster were investigated. He concluded that there is only marginal evidence in favor of a trend between the gas metallicity and the density of the environment. Most of the galaxies in his sample appear to follow to the general luminosity – metallicity relation for dwarf galaxies. Similar results were obtained by Lee et al. (2007), who found no pronounced dependence of the luminosity–metallicity, metallicity–gas fraction, and metallicity – tidal index diagrams on positive or negative tidal indices of dwarf irregular galaxies in nearby galaxy groups of different environmental densities.

Mouhcine et al. (2007) investigated the dependence of gas-phase chemical properties on stellar mass and environment using a sample of 37866 SDSS galaxies in the redshift range of $0.040 \lesssim z \lesssim 0.085$. They found that galaxies show a marginal increase in chemical enrichment level at a fixed stellar mass in denser environments. They concluded that the evolution of star-forming galaxies is driven primarily by their intinsic properties and is largely independent of their environment over a large range of local galaxy densities.

Ellison et al. (2009) found that cluster galaxies in locally rich environments have higher median metallicities by up to $\sim$ 0.05 dex than those in locally poor environments. Hughes et al. (2013) considered the relationship between stellar mass and metallicity for 260 nearby late-type galaxies in different environments, from isolated galaxies to Virgo cluster members. They found that the mass – metallicity relation is nearly independent of environment and concluded that internal evolutionary processes, rather than environment effects, play a key role in shaping the mass – metallicity relation.

Peng & Maiolino (2014) found that there is a strong dependence on environmental density for star-forming satellites (i.e., all galaxy members of groups/clusters that are not located at the centre) and that there is no correlation for galaxies located at the centre. Darvish et al. (2015) studied the properties of a sample of 28 star-forming galaxies in a large filamentary structure at $z \sim 0.53$ (using Keck spectroscopic data) and compared them with a control sample of 30 field galaxies. They found that, on average, star-forming galaxies in filaments are more metal-enriched ($\sim 0.1 - 0.15$ dex).

Shimakawa et al. (2015) considered the environmental dependence of gaseous metallicities at redshifts of $z = 2.2$ and 2.5 and found that the objects with masses below $10^{11} M_{\odot}$ tend to be more chemically enriched than their field counterparts at $z = 2.2$. Valentino et al. (2015) investigated the environmental effect on the metal enrichment of star-forming galaxies in a cluster at redshift $z = 1.99$. They found that the cluster's star-forming galaxies in the mass range of $10 \lesssim \log M \lesssim 11$ are up to 0.09 – 0.25 dex more metal-poor than their field counterparts, depending on the adopted calibration for the abundance determinations.

Gupta et al. (2016) determined the abundances in galaxies of two galaxy clusters at redshifts $z \sim 0.35$. They found for one cluster that the galaxy abundance decreases as a function of projected cluster-centric distance. The galaxies of this cluster are shifted towards higher metallicity by a mean value of 0.2 dex compared to the local reference sample at a given mass. The galaxies of another cluster exhibit a bimodal radial abundance distribution, with one branch showing a high galaxy metallicity near the centre of the cluster and negative radial gradient and the other branch showing a low galaxy metallicity at the cluster centre and positive radial gradient. Gupta et al. (2016) suggested that the lower branch galaxies belong to a merging sub-sluster and/or are interloper galaxies.

Looking at it from another angle, voids are the most underdense regions in the universe where galaxy evolution will have progressed without any significant influence of the environment. A number of very low-metallicity galaxies have been revealed within void environments (Pustilnik et al. 2013). The nebular metallicities of two dwarf galaxies in the Local Void were measured by Nicholls et al. (2014). They find that the metallicities in both galaxies are typical for galaxies of that size. Kreckel et al. (2015) measured gas-phase oxygen abundances and gas content for eight dwarf galaxies located within the lowest density environments of seven void galaxies and for a sample of isolated dwarf galaxies in average density environments. They find no significant difference between these void dwarf galaxies and the isolated dwarf galaxies. They noted that while the sample is too small to draw strong conclusions, their result suggests that the chemical evolution of dwarf galaxies proceeds independently of the large-scale environment. Beygu et al. (2016) studied the properties of 59 void galaxies and noted that their sample consists of high metallicity galaxies as well as galaxies of low metallicity.

We find for a large sample of galaxies that the oxygen and nitrogen abundances tend to be slightly higher in galaxies located in volumes with a high concentration of galaxies. The scatter in the abundances is large at any concentration of galaxies (at any density of the environment), i.e., galaxies with both enhanced and reduced abundances can be found at any density of the environment. Thus, our result confirms the conclusions of the previous studies that environmental effects do not play a key role in the chemical evolution of galaxies.

5 SUMMARY

We examined the influence of the environment on the abundances of late-type galaxies of masses of $10^{9.1}$ $M_{\odot}$ to 10^{11} $M_{\odot}$ with redsifts up to $z = 0.1$ from the Sloan Digital Sky Survey (SDSS). The oxygen and nitrogen abundances were estimated through our recent calibrations and are compatible to the T_e-based metallicity scale in H II regions. Galaxies with reliable stellar masses and oxygen and nitrogen abundances were extracted from the full sample.

The obtained oxygen abundance – galaxy mass (O/H – M) and the nitrogen abundance – galaxy mass (N/H – M) diagrams reproduce the known evolution of galactic abundances with mass and redshift.

The oxygen and nitrogen abundances increase with increasing mass and with decreasing redshift, and the X/H – M relations flattens out at the massive end.

The rate of change of the chemical abundances in galaxies at the present epoch decreases with increasing masses (the downsizing effect).

The rate of change of nitrogen abundance with redshift and stellar mass is higher than that for oxygen.

We studied the influence of the environmental density on the overabundance of oxygen and nitrogen and investigated the deviation of these abundances from the abundance – galaxy mass relation. The environmental density was specified by the number of neighbouring galaxies within a region in projected distance – redshift difference space. Five different values of the projected distance were considered: R_0 = 1 Mpc, 2 Mpc, 3 Mpc, 4 Mpc, and 5 Mpc. The redshift differences take into account the change of redshift with distance equal to the adopted R_0 and the peculiar velocities of galaxies V_p. Three peculiar velocities were considered: V_p = 1000 km s^{-1}, 500 km s^{-1}, and 100 km s^{-1}.

We find that the influence of the environment on the chemical abundances of galaxies is most pronounced for galaxies of masses of $10^{9.1}$ M$_\odot$ to $10^{9.6}$ M$_\odot$. The galaxies in the densest environments can show an abundance excess larger than about $\sim$ 0.05 dex in oxygen (based on the median value for 101 galaxies with the densest environments) and around $\sim$ 0.1 dex in nitrogen above the mean. The overabundance decreases with increasing galaxy mass and with decreasing environmental density.

The overabundance in galaxies in dense local environments (at R_0 = 1 Mpc) is higher than that of galaxies in dense extended environments (at R_0 = 5 Mpc), i.e., the oxygen overabundance is more sensivite to the local than to the extended environment density.

Since only a small fraction of galaxies are in high-density environments then they do not have a significant influence on the general X/H – M relation. The metallicity – mass relations for isolated galaxies and galaxies having neighbours are similar to each other. The mean shift of non-isolated galaxies around the metallicity – mass relation traced by the isolated galaxies is less than $\sim$ 0.01 dex for oxygen and less than $\sim$ 0.02 dex for nitrogen. The scatter in the overabundances is large at any environmental density, i.e., galaxies with both enhanced and reduced abundances can be found at any density of the environment. This suggests that environmental effects do not play a key role in the chemical evolution of late-type galaxies. This conclusion has been reached in a number of previous studies, and our results confirm that conclusion.

ACKNOWLEDGEMENTS

We are grateful to the referee for his/her constructive comments.
L.S.P., I.A.Z. and E.K.G. acknowledge support in the framework of Sonderforschungsbereich SFB 881 on "The Milky Way System" (especially subproject A5), which is funded by the German Research Foundation (DFG).
L.S.P. and I.A.Z.acknowledge support of the Volkswagen Foundation under the Trilateral Partnerships grant No. 90411.
L.S.P. and I.A.Z. thank for the hospitality of the Astronomisches Rechen-Institut at Heidelberg University where part of this investigation was carried out.
This work was partly funded by the subsidy allocated to Kazan Federal University for the state assignment in the sphere of scientific activities (L.S.P.).
Funding for the SDSS and SDSS-II has been provided by the Alfred P. Sloan Foundation, the Participating Institutions, the National Science Foundation, the U.S. Department of Energy, the National Aeronautics and Space Administration, the Japanese Monbukagakusho, the Max Planck Society, and the Higher Education Funding Council for England. The SDSS Web Site is http://www.sdss.org/.

REFERENCES

Ade P.A.R., Aghanim N., Armitage-Caplan C., et al., (Planck Collaboration XVI), 2014, A&A, 571, A16
Ade P.A.R., Aghanim N., Arnaud M., et al., (Planck 2015 results. XIII. Cosmological parameters), 2016, A&A, 594, A13
Ahn C. P., Alexandroff R., Allende Prieto C., et al. 2012, ApJS, 203, 21
Alam S., Albareti F. D., Allende Prieto C., et al. 2015, ApJS, 219, 12
Alpaslan M., Robotham A.S.G., Driver S., et al., 2014, MNRAS, 438, 177
Andrews B.H., Martini P., 2013, ApJ, 765, 140
Annibali F., Tosi M., Pasquali A., Aloisi A., Mignoli M., Romano D., 2015, AJ, 150, 143
Argudo-Fernández M., Verley S., Bergond G., Duarte Puertas S., Ramos Carmona E., Sabater J., Fernández Lorenzo M., Espada D., Sulentic J., Ruiz J.E., Leon S., 2015, A&A, 578, A110
Baldwin J.A., Phillips M.M., Terlevich R., 1981, PASP, 93, 5
Balogh M.L., Baldry I.K., Nichol R., Miller C., Bower R., Glazebrook K., 2004, ApJ, 615, L101
Berg D.A., Skillman E.D., Marble A.R., et al., 2012, ApJ, 754, 98
Beygu B., Kreckel K., van der Hulst J.M., Jarrett T.H., Peletier R., van der Weygaert R., van Gorkom J.H., Aragon-Calvo M.A., 2016, MNRAS, 458, 394
Bond J.R., Kofman L., Pogosyan D., 1996, Nature, 380, 603
Bothwell M.S., Maiolino R., Kennicutt R., Cresci G., Mannucci F., Marconi A., Cicone C., 2013, MNRAS, 433, 1425
Brough S., Croom S., Sharp R., et al., 2013, MNRAS, 435, 2903
Bruzual G., Charlot S., 2003, MNRAS, 344, 1000
Chen Y-M., Kauffmann G., Tremonti C.A., et al., 2012, MNRAS, 421, 314
Cowie L.L., Songaila A., Hu E.M., Cohen J.G., 1996, AJ, 112, 839
Cowie L.L., Barger A.J., 2008, ApJ, 686, 72
Croxall K., Pogge R.W., Berg D.A., Skillman E.D., Moustakas J., 2016, ApJ, 830, 4
Daddi E., Elbaz D., Walter F., Bournaud F., Salmi F., Carilli C., Dannerbauer H., Dickinson M., Monaco P., Riechers D., 2010, ApJ, 714, L118
Darvish B., Mobasher B., Sobral D., Hemmati S., Nayyeri H., Shivaei I., 2015, ApJ, 814, 84
Dawson K. S., Schlegel D. J., Ahn C. P., et al. 2013, AJ, 145, 10
de Lapparent V., Geller M.J., Huchra J.P., 1986, ApJ, 302, L1
Dressler A., 1980, ApJ, 236, 351
Edmunds M.G., Pagel B.E.J., 1978, MNRAS, 185, 77
Ellison S.L., Patton D.R., Simard L., McConnachie A.W., 2008, ApJ, 672, L107
Ellison S.L., Simard L., Cowan N.B., Baldry I.K., Patton D.R., McConnachie A.W., 2009, MNRAS, 396, 1257
Erb D.K., Shapley A.E., Pettini M., Steidel C.C., Reddy N.A., Adelberger K.L., 2006, ApJ, 644, 813
Freedman W.L., Madore B.F., Gibson B.K., et al., 2001, ApJ, 553, 47
Fuse C., Marcum P., Fanelli M., 2012, AJ, 144, 57
Heavens A., Panter B., Jimenez R., Dunlop J., 2004, Nature, 428, 625
Henry R.B.C., Edmunds M.G., Köppen J., 2000, ApJ, 541, 660
Hughes T.M., Cortese L., Boselli A., Gavazzi G., Davies J.I., 2013, A&A, 550, A115
Garnett D.R., 2002, ApJ, 581, 1019
Gavazzi G., 1993, ApJ, 419, 469
Gott J.R. III, Juríc M., Schlegel D., Hoyle F., Vogeley M., Tegmark M., Bahcall N., Brinkmann J., 2005, ApJ, 624, 463
Grebel E. K., Gallagher J. S. III, Harbeck D. 2003, AJ, 125, 1926
Gupta A., Yuan T., Tran K.-V. H., Martizzi D., Taylor P., Kewley L.J., 2016, astro-ph 1608.06289
Guseva N.G., Papaderos P., Meyer H.T., Izotov Y.I., Fricke K.J., 2009, A&A, 505, 63
Izotov Y.I., Thuan T.X., Lipovetsky V.A., 1994, ApJ, 435, 647
Izotov Y.I., Thuan T.X., 1999, ApJ, 511, 639
Izotov Y.I., Guseva N.G., Fricke K.J., Henkel C., 2015, MNRAS, 451, 2251
Kacprzak G.G., Yuan T., Nanayakkara T., Kobayashi C., Tran K.-V.H., Kewley L.J., Glazebrook K., Spitler L., Taylor P., Cowley M., Labbe I., Straatman C., Tomczak A., 2015, ApJ, 802, 26L
Kannappan S.J., Gawiser E., 2007, ApJ, 657, L5

Kauffmann G., Heckman T.M., Tremonti C., et al., 2003, MNRAS, 346, 1055
Kennicutt R.C., 1998, Annual. Rev. of A&A, 36, 189
Kennicutt R.C., Evans N.J., 2012, Annual. Rev. of A&A, 50, 531
Kewley L.J., Jansen R.A., Geller M.J., 2005, PASP, 117, 227
Kreckel K., Croxall K., Groves B., van de Weygaert R., Pogge R.W., 2015, ApJ, 798, L15
Lacerna I., Hernández-Toledo H.M., Avila-Reese V., Abonza-Sane, del Olmo A., 2016, A&A, 588, A79
Lara-López M.A., Cepa J., Bongiovanni A., Pérez García A.M., Ederoclite A., Castaǹeda H., Fernández Lorenzo M., Pović M., Sánchez-Portal M., 2010, A&A, 521, L53
Lee H., Zucker D.B., Grebel E.K. 2007, MNRAS, 376, 820
Lequeux J., Peimbert M., Rayo J. F., Serrano A., Torres-Peimbert S. 1979, A&A, 80, 155
Lynden-Bell D., Faber S.M., Burstein D., Davies R.L., Dressler A., Terlevich R.J., Wegner G., 1988, ApJ, 326, 19
Maier C., Lilly S.J., Ziegler B.L., Contini T., Pérez Montero E., Peng Y., Balestra I., 2014, ApJ, 792, 3
Maiolino R., Nagao T., Grazian A., et al., 2008, A&A, 488, 463
Mannucci F., Cresci G., Maiolino R., Marconi A., Gnerucci A., 2010, MNRAS, 408, 2115
Maraston C., Strömbäck G., Thomas D., Wake D.A., Nichol R.C., 2009, MNRAS, 394, L107
Mouhcine M., Baldry I.K., Bamford S.P., 2007, MNRAS, 382, 801
Moustakas J., Kennicutt R.C., Tremonti C.A., Dale D.A., Smith J.-D.T., Calzetti D., 2010, ApJS, 190, 233
Nicholls D.C., Jerjen H., Dopita M.A., Basurah H., 2014, ApJ, 780, 88
Pagel B.E.J., 1997, Nucleosynthesis and Chemical Evolution, Cambridge, Cambridge Univ. Press
Peng Y., Maiolino R., 2014, MNRAS, 438, 262
Pilyugin L.S., Mollá M., Ferrini F., Vílchez J.M., 2002, A&A, 383, 14
Pilyugin L.S., Thuan T.X., Vílchez J.M., 2003, A&A, 397, 487
Pilyugin L.S., Vílchez J.M., Contini T., 2004, A&A, 425, 849
Pilyugin L.S., Thuan T.X., Vílchez J.M., 2006, MNRAS, 367, 1139
Pilyugin L.S., Thuan T.X., Vílchez J.M., 2007, MNRAS, 376, 353
Pilyugin L.S., Thuan T.X., 2011, ApJ, 726, 23P
Pilyugin L.S., Lara-López M.A., Grebel E.K., Kehrig C., Zinchenko I.A., López-Sánchez Á.R., Vílchez J.M., Mattsson L., 2013, MNRAS, 432, 1217
Pilyugin L.S., Grebel E.K., Kniazev A.Y., 2014, AJ, 147, 131
Pilyugin L.S., Grebel E.K., 2016, MNRAS, 457, 3678
Poggianti B.M., Smail I., Dressler A., Couch W.J., Barger A.J., Butcher H., Ellis R.S., Oemler A., 1999, ApJ, 518, 576
Pustilnik S.A., Martin J.-R., Lyamina Y.A., Kniazev A.Y., 2013, MNRAS, 432, 2224
Riess A.G., Macri L.M., Hoffmann S.L., et al., 2016, ApJ, 826, 56
Sánchez S.F., Rosales-Ortega F.F., Iglesias-Páramo J., et al. 2014, A&A, 563, 49
Shapley H., 1930, Bull. Harvard Obs., 874, 9
Sheth R.K., Diaferio A., 2011, MNRAS, 417, 2938
Shields G.A., Skillman E.D., Kennicutt R.C., 1991, ApJ, 371, 82
Shimakawa R., Kodama T., Tadaki K.-I., Hayashi M., Koyama Y., Tanaka I., 2015, MNRAS, 448, 666
Skillman E.D., Kennicutt R.C., Shields G.A., Zaritsky D., 1996, ApJ, 462, 147
Spector O., Brosch N., 2016, MNRAS, 456, 885
Steidel C.C., Rudie G.C., Strom A.L., et al., 2014, ApJ, 795, 165
Stoughton C., Lupton R. H., Bernardi M., et al. 2002, AJ, 123, 485
Thuan T.X., Pilyugin L.S., Zinchenko I.A., 2010, ApJ, 712, 1029
Tomczak A.R., Quadri R.F., Tran K-V.H., et al., 2016, ApJ, 817, 118
Tremonti C.A., Heckman M., Kauffmann G., et al., 2004, ApJ, 613, 898
Valentino F., Daddi E., Strazzullo V., et al., 2015, ApJ, 801, 132
van der Wel A., 2008, ApJ, 675, L13
van Zee L., Salzer J.J., Haynes M.P., O'Donoghue A.A., Balonek T.J., 1998, AJ, 116, 2805
Vila-Costas M.B., Edmunds M.G. 1992, MNRAS, 259, 121
Vílchez J.M., 1995, AJ, 110, 1090
Wijesinghe D.B., Hopkins A.M., Brough S., et al., 2012, MNRAS, 423, 3679
Whitford A.E., 1958, AJ, 63, 201
York D.G., Adelman J., Anderson J.E., et al., 2000, AJ, 120, 1579
Zahid H.J., Geller M.J., Kewley L.J., Hwang H.S., Fabricant D.G., Kurtz M.J., 2013, ApJ, 771, L19
Zaritsky D., Kennicutt R.C., Huchra, J.P., 1994, ApJ, 420, 87
Zeldovich I.B., Einasto J., Shandarin S.F., 1982, Nature, 300, 407
Zhang W., Li C., Kauffmann G., Zou H., Catinella B., Shen S., Guo Q., Chang R., 2009, MNRAS, 397, 1243